A Dissertation on

DESIGN, MODELING AND SIMULATION OF RF MEMS TUNABLE BAND PASS FILTER IN Ku BAND

Submitted to

Delhi Technological University

(Formerly Delhi college of Engineering)

Govt. of NCT of Delhi

Main Bawana Road, Delhi-110042

In the partial fulfillment of the requirements of the degree

of

MASTER OF TECHNOLOGY

in

MICROWAVE AND OPTICAL COMMUNICATION ENGINEERING

By

ROHIT KUMAR

(2K14/MOC/15)

Under the Guidance

of

Dr. Priyanka Jain

Assistant Professor

Department of Electronics and communication

DTU, DELHI

DECLARATION

I, **Rohit Kumar**, hereby declare that the work which is being presented in the thesis entitled, "**Design, Modeling and Simulation of RF MEMS Tunable Band Pass Filter in Ku Band**" being submitted by me in the partial fulfilment of the requirement for the award of degree of Master of Technology in **Microwave and Optical Communication Engineering**, Delhi Technological University, Delhi, India is an authentic record of my own work carried out under the guidance of Mr. Updesh Sharma, Scientist , SSPL DRDO, and Dr. Priyanka Jain, Assistant Professor, DTU. The matters embodied in this record have not being submitted by me for the award of any other degree.

Date:

Rohit Kumar
2K14/MOC/15
DTU, Delhi

ACKNOWLEDGEMENT

Firstly, I would like to thank Mr. Updesh Sharma, from the Si MEMS department of SSPL, DRDO, who has guided me throughout the project. Her enthusiasm for science has been my motivation till the end. Her knowledge of the subject and her innovative ideas has been a great resource and inspiration. It was because of her constant guidance that I was able to complete this work.

I would never have the energy to work at SSPL if it were not for my post graduate mentor and supervisor Dr. Priyanka Jain. It was the fundamentals that she taught me that enabled me to understand the problems that I faced during my project. He always had time to spare for me and guide me through the right path. He was the one who taught me to have a research oriented approach to my learning. He always inspired me to be well updated in anything that I am learning.

I would like to thank Mr. Prem R.Chadha, Head of Department, Electronics and communication, Delhi Technological University for recommending me to work in an esteemed institute like SSPL. Without him I would never have been able to do a project like this in the first place. His energy and youthfulness has always made me challenge myself and be devoted to the work I am doing. His smiling face has always been a great comfort whenever I used to be tensed or worried.

I would like to thank Dr. Kapil Kumar Jain, Head of Department of SI MEMS Department, SSPL for giving me the opportunity to work in SSPL. It was a great experience for me and has given me a whole new perspective to learning. His knowledge and hard working nature has been a source of great inspiration to me.

Finally, I am thanking my parents and all my friends for their support and encouragement. They have been with me even in difficult times. Their advice and support is something that has always kept me going. They are the ones who have always given smiles in my life. I am always grateful to them.

Thank you,

Rohit Kumar

CERTIFICATE

This is to certify that the M.Tech. synopsis entitled **"Design, Modeling and Simulation of RF MEMS Tunable Band Pass Filter in Ku band"**. submitted by **Rohit Kumar (2K14/MOC/15)** in fulfilment of the requirement for the major project thesis during M.Tech., Delhi Technological University (Formerly Delhi College of Engineering) is an authentic record of the candidate's own work which is to be carried out by him under our guidance. The information and data enclosed in this dissertation is original.

Dr. Priyanka Jain
(Supervisor)
Assistant Professor
Electronics and Communication
Delhi Technological University
Delhi – 110042

Mr. Updesh Sharma
(Supervisor)
Scientist 'E'
Solid State Physics Laboratory
DRDO
Delhi- 110054

Head of Department
Electronics and Communication
Delhi Technological University
Delhi - 11004

ABSTRACT

Numerous communication systems require a filter with tunable frequency and bandwidth states. A common filter bank with multi-throw switch is available but it takes alot of space and has high losses. To solve such problem, tunable band pass filters based on MEMS technology are being widely studied. It is expected that MEMS technology can bring much improvement to the tade off between tuning range and losses in filter design. One of such approach is the DMTL configuration. A distributed MEMS transmission line (DMTL) is used to realize a transmission-line with a voltage-variable electrical length for microwave circuits. The DMTL is a coplanar waveguide periodically loaded with continuously-variable MEMS capacitors which is realized with shunt switches or bridges. This dissertation is focused on designing; modeling and simulation of tunable band pass filter in Ku band around 15 GHz that is to be fabricated on 270 um thick silicon ($\boldsymbol{\varepsilon_r} = 11.9$) substrate using capacitive coupled DMTL sections as variable shunt resonators. As per simulated results, the tunability of 2.9% has been achieved with minimum insertion loss 3.87dB, and bandwidth variation of 8.3-8.5% in tuning range.

INDEX

CONTENTS	PAGE NO.
Declaration	**i**
Acknowledgement	**ii**
Certificate	**iii**
Abstract	**iv**
Index	**v**
List of Tables	**vii**
List of Figures	**viii**
Chapter 1 : Introduction	**1**
1.1 Overview	1
1.2 The beginning of RF MEMS	2
1.5 Application area of RF MEMS and replacement strategies	4
1.6 Objective of the project	6
Chapter 2 : Literature Review	**7**
2.1 Introduction	7
2.2 MEMS Tunable Capacitors	7
2.2.1 Series Switch	8
2.2.2 Shunt Switch	9
2.3 RF MEMS configurations	10
2.4 DMTL	11
2.6 RF MEMS Tunable Band Pass Filter	12
2.6.1 Analog Tuning of a MEMS Band-Pass Filter	13
2.6.2 Digital Tuning of an RF MEMS Filter	14
Chapter 3 : Microwave Filter Theory	**16**
3.1 Introduction	16
3.2 Filter Design Method	16
3.2.1 Periodic Structure	16
3.2.2 Image Parameter Method	17
3.2.3 Insertion Loss Method	17
3.2.4 Stepped Impedance Method	22
3.2.5 Coupled Line Filter	22
3.2.6 Band Pass Filter using Capacitively Coupled Resonators	23

Chapter 4 : Electromagnetic Modeling and Designing of the Filter	24
4.1 Introduction	24
4.2 Electromagnetic model of the MEMS capacitor	24
4.3 Analytically calculated model parameters for DMTL section	28
4.4 Design of single pole band pass filter	29
Chapter 5 : Electromechanical Modeling of the Filter	**31**
5.1 Introduction	31
5.2 Static Analysis	31
5.2.1 Spring Constant of Fixed-Fixed beam shunt switch	31
5.2.2 Electrostatic actuation analysis	34
5.3 Electromechanical Simulation Results	35
Chapter 6 : RF Simulation of Tunable Band Pass Filter	**40**
6.1 Introduction	40
6.2 RF MEMS Tunable Band Pass Filter	40
6.2.1 Design	40
6.2.2 RF Characterization by HFSS v13 Simulation	41
Chapter 7 : Conclusion and Scope of Future Work	**44**
7.1 Conclusion	44
7.2 Work to be carried out and its future scopes	45
References	**46**

List of Tables

1.1. Application areas of MEMS Switches, Varactors and High-Q Inductors, 4

1.4. RF MEMS Replacement Strategies, 5

2.1. Typical design parameters of conventional RF MEMS shunt switch, 10

2.2 Different configuration of MEMS devices, 10

3.1. Elemental values for maximally flat low pass filter prototype (g_o=1, c_o=1, N=1 to 10), 18

3.2. Elemental values for maximally flat low pass filter prototype (g_o=1, c_o=1, N=1 to 10), 19

4.1. MEMS capacitance variation with air gap, 26

4.2. MEMS Inductance variation with air gap, 26

4.3. Simulated Static capacitance of the designed MEMS capacitor, 27

4.4. Summary of $C_{i-1, i}$ and lelec, 30

5.1. Summary of spring constant for 20um x 300 um fixed-fixed beam , 34

5.2. Relation between residual stress and Pull in voltage, 35

5.3. Relation of displacement with applied voltage for given air gap, 37

6.1. Design parameters of capacitively coupled DMTL resonator, 41

6.2 Relation of central frequency and losses with actuation, 42

6.3. Relation of capacitance and relative 3dB bandwidth with actuation, 42

6.4 Relation of central frequency and losses with actuation, 43

6.5. Relation of capacitance and relative 3dB bandwidth with actuation, 43

List of Figures

1.1. A class of filter bank, 2

1.2. Tunable filter Linkage, 3

2.1. Broadside MEMS-series switches, 8

2.2. MEMS capacitive shunt switch, 9

2.3. A DC-contact MEMS shunt switch with two pull-down electrodes, 9

2.4. (a) DMTL layout, 12

(b) Lumped t-line model of single shunt switch section, 12

2.5. Photograph of fabricated three-pole MEMS tunable band-pass filter, 13

2.6. Measured S parameter of capacitively coupled MEMS tunable filter, 13

2.7. Micrograph of the fabricated MEMS miniature filter, 14

2.8. Measured and simulated S parameters of the miniature tunable filter, 14

2.9. Layout of the UHF five-pole filter, 15

2.10. UHF responses, 15

3.1. (a) Periodic stub on microstrip line, 16

(b) Periodic diaphragm in waveguide, 16

3.2. The process of filter design by insertion loss method, 17

3.3. Attenuation verses normalized frequency for maximally flat filter prototype, 18

3.4. Attenuation verses normalized frequency for Equal ripple filter prototype, 19

3.5. (a) Prototype begins with a shunt element, 20

(b) Prototype begins with a series element, 20

3.6. Band pass circuit, 22

3.7. Microstrip layout of stepped impedance filter, 22

3.8. Layout of coupled line filter, 22

3.9. (a) Capacitive gap coupled resonator band pass filter, 23

(b) Transmission line model, 23

4.1. The cross sectional view of the MEMS capacitor, 24

4.2. Equivalent CLR model of the switched capacitor, 25

4.3. (a) MEMS capacitive shunt switch in up-state, 26

(b) MEMS capacitive shunt switch in actuated-state, 26

4.4. Simulated result of Capacitance verses air gap, 27

4.5. Schematic and equivalent circuit of a DMTL, 28

4.6. (a) Topology of single pole capacitively coupled tunable filter, 29

(b). Layout tunable filter in coplanar-waveguide form, 29
4.9. Coupling capacitors, 30
5.1. Fixed–fixed beam with the force evenly distributed about the center of the beam, 31
5.2. (a) Spring Constant Due to Beam Stiffness, 33
(b) Spring Constant Due to residual stress, 33
(c) Total spring constant, 33
5.3. Beam height versus applied voltage, 34
5.4. (a) Process definition of design, 36
(b) Material properties definition, 36
(c) Required Actuator design, 37
5.5. Dynamic view of shunt bridge, 39
6.1. (a) Top view of the designed filter, 40
(b) Three dimensional view of the structure, 41
6.2. S-parameters (dB) vs. Frequency (GHz) [optimization 1]' 42
6.3. S-parameters (dB) vs. Frequency (GHz) [optimization 2]' 43

CHAPTER 1
INTRODUCTION

1.1. OVERVIEW

The electromagnetic spectrum is the range of every conceivable frequencies of electromagnetic radiation and can be partitioned into a number of frequency bands. The frequency band of our concern is radio frequency of microwave range. Microwave frequency ranges from 300 MHz to 300 GHz. Microwave finds various applications in

(1) Telecommunications
(2) Radar
(3) Navigation
(4) Space communication
(5) Sensing
(6) Medical instrumentation and treatment etc.

The primary function of a filter is to either separate or join diverse frequencies and segregate between needed and undesirable frequencies. This makes them useful in order to confine the RF/Microwave signals within the assigned spectral limits. They can be realized in a variety of ways which include waveguide, coaxial or microstrip lines, MEMS and so on. More stringent requirements are being placed on filters as the developing applications require more functionality. These prerequisites may include

(1) Higher Performance
(2) Smaller Size
(3) Lighter weight
(4) Lower cost

As the multifunctional and multiband requirements are increasing day by day, tunable filters have become a crucial part of present communication systems. Numerous systems require a filtering system with switchable/tunable frequency and/or bandwidth states. A common filter bank is outlined in Fig.1.1 which takes up a lot of space and multi-throw switches have high losses. In recent years, tunable band-pass filters based on MEMS technology have been widely studied. It is expected that MEMS technology can bring much improvement to the tradeoffs

between tuning range and losses in filter designs. Both the capacitive switch and the metal-contact switch can be used to construct MEMS tunable band-pass .This thesis is also an attempt to design a tunable filter using capacitively coupled DMTL based resonator. Cascading concept has been used to improve the rejection while designing the filter. Also this thesis has covered all areas associated with the designed filter starting by mechanical modeling, electrical modeling and concluded by simulated results with its possible applications as tunable filter in communication system. To design such filters, inter linked diagram has been shown in Fig.1.2.

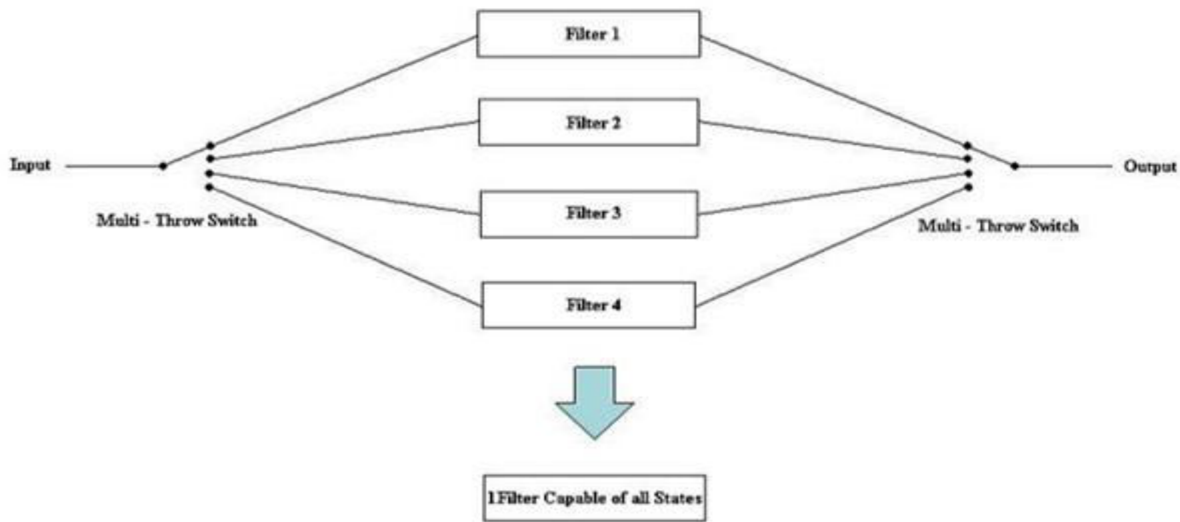

Fig.1.1. A class of filter bank

1.2. THE BEGINNING OF RF MEMS

MEMS have been developed since 1970s for sensor devices. In 1980, MEMS switches have been developed for low frequency applications and remained a laboratory concern for long time. Later in 1990-1991, Dr Larry Larson at the Hughes Research lab California developed a MEMS switch (or varactor) for microwave application, despite poor yield; it demonstrated excellent performance up to 50 GHz, far better than achieved with GaAs devices. RF MEMS has seen an amazing growth in the past 10 years due to its immense commercial and defense potential. The reason is that while there were tremendous advances in GaAs HEMT devices (high-electron mobility transistor) and in silicon CMOS (complementary metal-oxide-semiconductor) transistors; there was barely an advance in semiconductor switching diodes from 1985 to 2000.

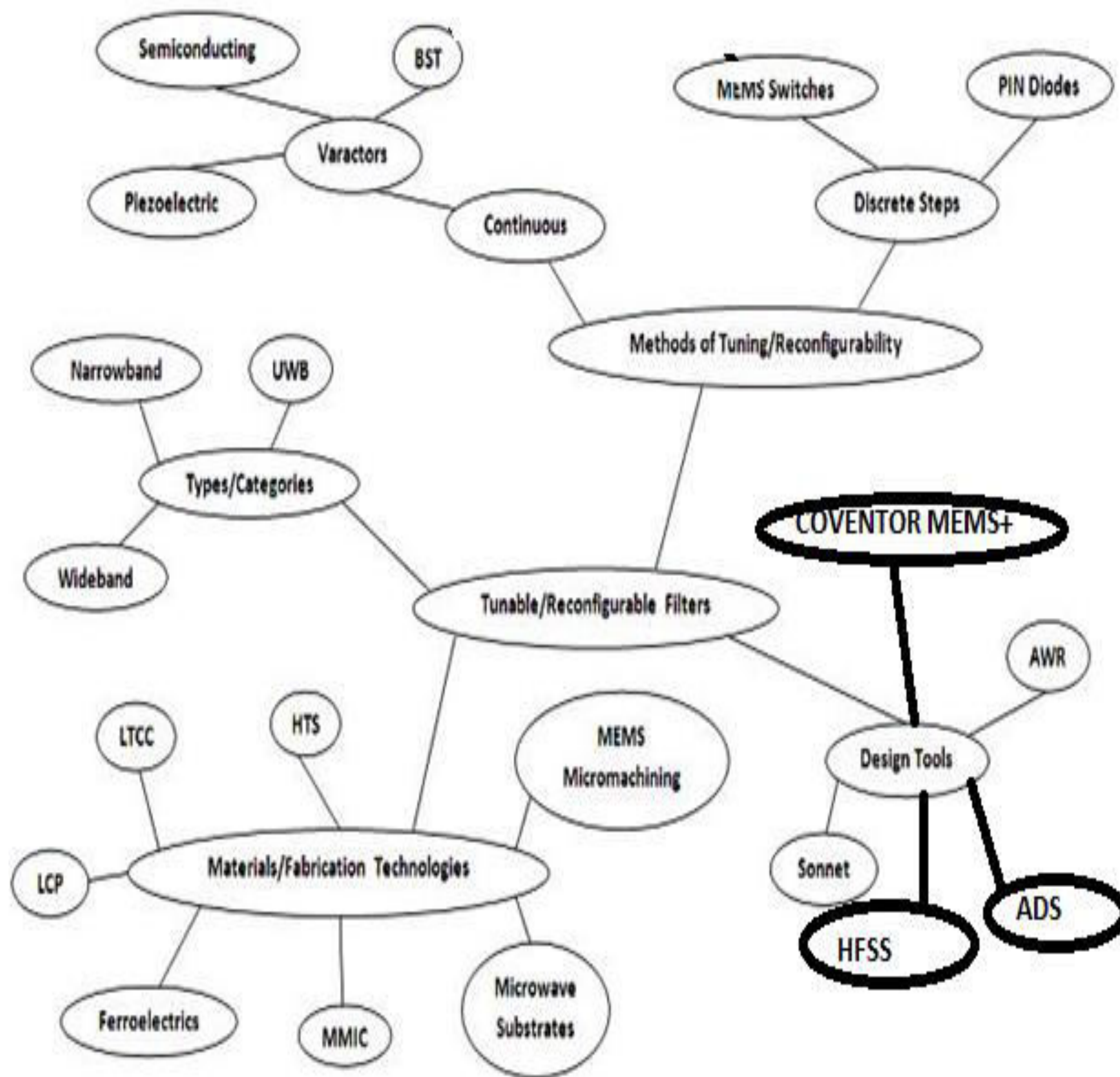

Fig. 1.2.Tunable filter Linkage

In 1980, the cutoff frequency of silicon CMOS transistors was around 500 MHz and is currently around 100 GHz. Also in 1980, the cutoff frequency of GaAs –HEMT devices was 10-20 GHz and is now above 800 GHz. However, the cutoff frequency of GaAs or InP p-i-n diodes improved from around 500 GHz in 1985 to only 2000 GHz in 2001. Clearly, a radical new

technology was needed to push the cut-off frequency of switching devices to 40,000 GHz for low-loss applications, and this was achieved with RF MEMS devices. One of the distinct areas of survey is in the field of RF micromechanical resonators and filters that use the mechanical vibrations of extremely small beams to achieve high-Q resonance at 0.01-200 MHz in vacuum. In this case, the mechanical movements are of the order of tens of angstroms. Very-high-Q resonators (>8000) have been fabricated using this technology up to 200 MHz, but two-pole filters have only been demonstrated up to 10 MHz . This technology still needs a lot of work before it is ready for commercial applications in miniature low frequency band filters [1].

1.3. APPLICATION AREAS OF RF MEMS AND REPLACEMENT STRATEGIES

Because of its outstanding isolation and insertion loss at microwave frequencies MEMS can replace the GaAs switches in cellular telephones resulting in much lower DC-power consumption and longer battery life. It can also be used in phase shifters, which are essential for modem telecommunication, automotive, and defense applications, in low-loss tunable circuits (matching networks, filters, etc.), and in high-performance instrumentation systems. Table1.3 and Table1.4 summarize the application areas of RF MEMS devices and the lifetime and number of cycles required.

Table1.3. Application areas of MEMS Switches, Varactors and High-Q Inductors

Area	System	Number of Cycles (Billions)	Years
Phased arrays	Communication systems (ground)	1-10	2-10
	(space)	10-100	2-10
	(airborne)	10-100	2-10
Phased arrays	Radar systems (Ground)	10-100	5-10
	(Space)	10-100	5-10
	(Missile)	0.2-10	1-5
	(Airborne)	1-100	5-10
	(Automotive)	1-10	5-10
Switching and Reconfigurable	Wireless communication (portable)	0.01-4	2-3
	(base station)	0.1-100	5-10

Networks	Satellite (Communication and radar) Airborne (Communication and radar) Instrumentation	0.1-1 0.1-10 10-100	2-10 2-10 10
Low-power Oscillators, filter and Amplifiers	Wireless communication (portable) Satellite (Communication and radar) Airborne (Communication and radar)	0.1 0.1-1 0.1-10	2-3 2-10 2-10

Table 1.4: RF MEMS Replacement Strategies

MEMS components	Subsystem	Replacement Strategy	Reasons
Switch	Transmitter Receiver	Possible in SPST , SPDT filter banks But Not soon for SPNT(N > 2)	Very low loss High reliability for low RF power Don't handle high RF power Reduce cost of SPDT and SPST
Switch	Switched antennas	Not soon	Must be able to handle high RF power
Inductor	Oscillator Power amplifier	Possible Possible	Low cost implementation Eliminate off chip inductor Still need higher Q MEMS inductor for matching network
Varactor	Oscillator	Possible/Not soon	Brownian noise problems in direct conversion receiver Possible in heterodyne receiver and/or mm wave oscillator
Varactor	Tunable filter	Possible	High Q MEMS results in low loss design Low inter modulation product

Varactor	Tunable matching network	Not soon /Possible	Must handle high RF power for antenna and power amplifier Possible in low power receiver application
MEMS filter	Filter	Not soon	Technology is still not ready even at 100 MHz Requires vacuum packaging
MEMS resonators	Oscillator	Possible	May replace crystal resonator if thermal stability solved Require Vacuum packaging

1.4. OBJECTIVE OF THE PROJECT

A distributed MEMS transmission line (DMTL) is used to realize a transmission-line with a voltage-variable electrical length for microwave circuits. The DMTL is a coplanar waveguide periodically loaded with continuously-variable MEMS capacitors. A tunable band pass filter has been designed on 270 µm thick silicon substrates using capacitively coupled DMTL sections as variable resonators. Issues for future improvement are discussed. So, the objective of the project can be summarized as under:-

- Design and simulation of voltage variable resonator length DMTL band pass filter in Ku band around 15 GHz.
- Achieving better insertion loss (S21) and return loss (S11)
- Electromagnetic modeling, electromechanical modeling and RF simulation of the design.

CHAPTER 2
LITERATURE REVIEW

2.1. INTRODUCTION

As mentioned in Chapter 1, micro electromechanical systems (MEMS) switches can be used to make tunable circuits, such as tunable capacitors, tunable filters, phase shifters, and matching networks. In this chapter tunable capacitors and tunable filters are discussed in detail.

2.2. MEMS TUNABLE CAPACITORS

In many modern wireless systems, such as low-noise amplifiers, harmonic frequency generators, and frequency controllers, a high-quality, stable, low-phase-noise voltage-controlled oscillators (VCOs) with a wide tuning range are essential elements. The tuning range of these VCOs must be large enough to cover the entire frequency band of interest. Tunable capacitors are the key elements in oscillators. Capacitance can be tuned or varied via electrical means, for example, by applying a tuning voltage, which makes the capacitance voltage-dependent, that is, C = C (V). Comparing semiconductor on-chip varactors, MEMS tunable capacitors have lower losses because of highly conductive thick metal layers used as structural material and air as a dielectric. A MEMS tunable capacitor also acts as a low-pass filter, and the interference between the capacitance variations and the applied RF signal remain small, thus offering excellent linearity. For a MEMS tunable capacitor, its quality factor (Q factor) can be defined as

$$Q = \frac{X_C - X_L}{ESR} \qquad 2.1$$

where X_C - X_L is the net reactance, ESR is the equivalent series resistance

From Eq. (2.1) it can be seen that as the resistance increases, Q decreases and resistive loss increases. Also, the inductance associated with the tunable capacitor will resonate at a frequency known as the electrical self resonance for the capacitor. The capacitor becomes unusable beyond the self-resonance frequency because the inductance dominates the total device impedance. Therefore, the inductance associated with a capacitor needs to be kept as low as possible. The self resonance should be much higher than the signal frequencies for which the tunable capacitor is designed [8]. MEMS capacitors can be tuned by adjusting the device’s physical parameters and dimensions via electromechanical means—electrostatic or thermal. After neglecting the

fringing fields, the capacitance of the capacitor with two electrodes of area a separated by a gap d can be written as

$$C = \frac{\varepsilon_o \varepsilon_r A}{d} \quad 2.2$$

where A = denotes the electrode area

d = the spacing between the plates

ε_o = the permittivity of free space

ε_r = the dielectric constant of the medium in between the two plates

Such tunable capacitors are based on MEMS switch design. There are two basic switches that are used for the purpose of variable capacitor design in RF to millimeter-wave circuits: the shunt switch and the series switch [1, 2].

2.2.1. SERIES SWITCH

There are two types of MEMS series switches: (i) the broadside series switch and (ii) the inline series switch. The actuation of the broadside switch is in a plane that is perpendicular to the transmission line, while the actuation of the inline switch is in the same plane as the transmission line. The actuation mechanism is achieved by using an electrostatic force between the top and bottom electrodes.

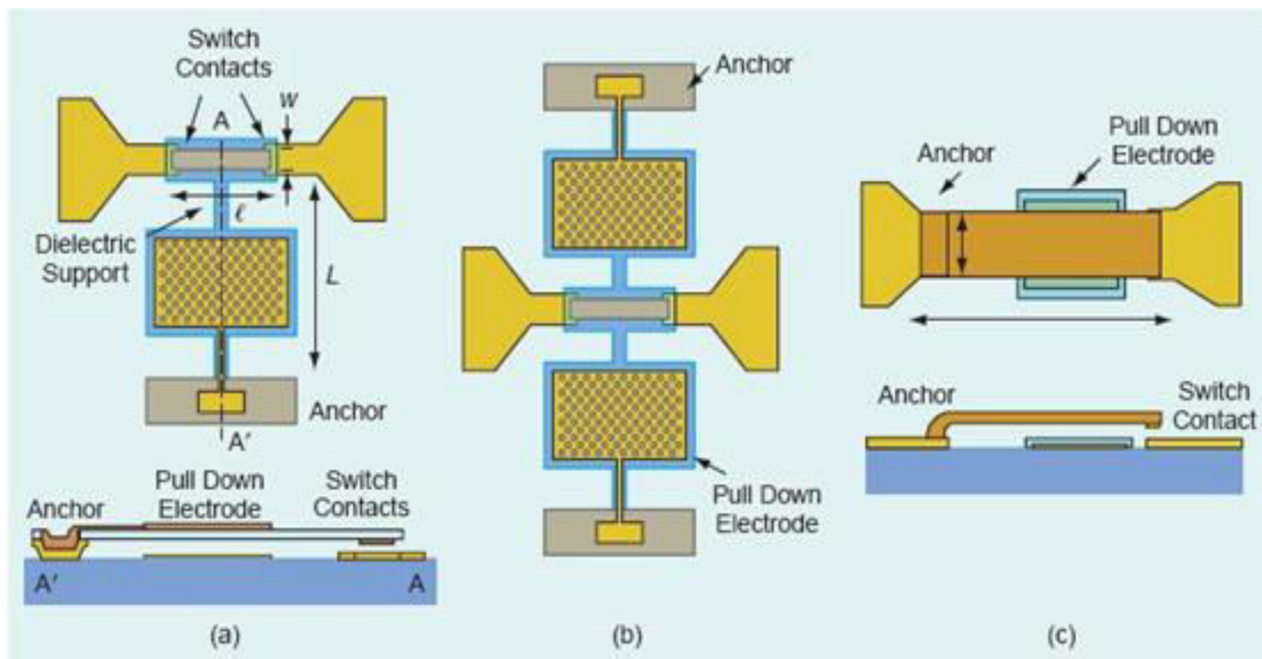

Fig.2.1. Broadside MEMS-series switches with (a) one electrode, (b) two electrodes, and (c) inline MEMS-series switches.

2.2.2. SHUNT SWITCH

There are different types of MEMS shunt switches, which provide different performance. Usually shunt switch is based on a fixed-fixed beam design. The anchors are connected to the CPW ground plane, and the membrane is grounded. The center electrode provides both the electrostatic actuation and the RF capacitance between the transmission line and the ground. When the switch is in the up state i.e. the zero biased state, it provides the low capacitance to the ground. When the switch is actuated by applying the controlled voltage .The capacitance starts increasing and at pull down voltage, this results in an excellent short circuit and high isolation at microwave frequencies.

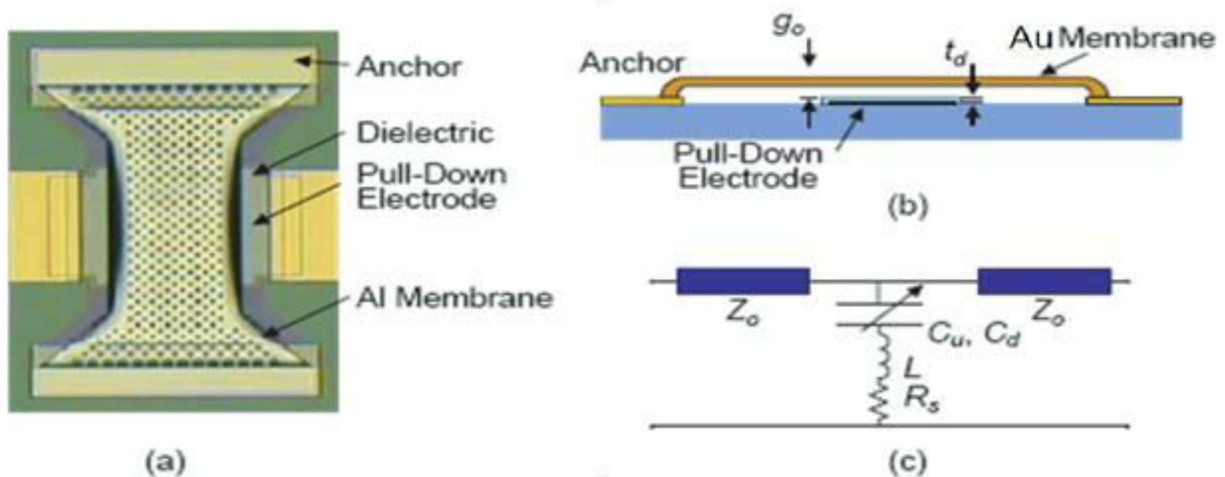

Fig.2.2. MEMS capacitive shunt switch: (a) Top-view, (b) Cross-sectional view and (c) electrical CLR model.

Sometimes instead of giving bias voltage to signal line, two pull down electrodes are as given in Fig. 2.3. Table 3.1 summarizes the range of typical values of design parameters for conventional switched capacitor modeling.

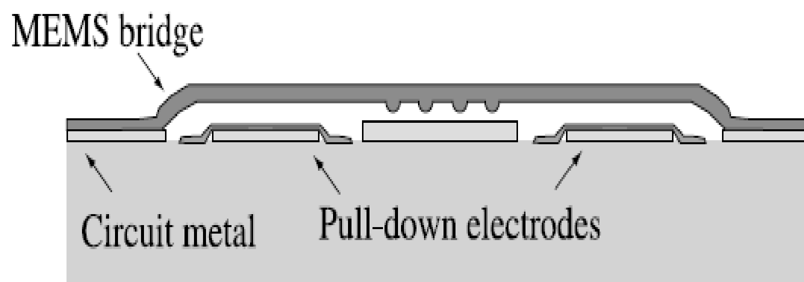

Fig.2.3. A DC-contact MEMS shunt switch with two pull-down electrodes

Table2.1.Typical design parameters of conventional RF MEMS shunt switch [1]

Parameters	Range of Typical Values
Bridge Length(L_b)	250-400(μm)
Bridge Width(w_{eb})	15-180(μm)
Bridge Thickness(t_{ab})	1.5-5(μm)
Dielectric Thickness(td)	1000-1500(Å)
Relative Dielectric Constant(r_{ed})	5.0-7.6
Capacitance Ratio(C_r)	40-500
Frequency of operation(f_r)	5-100(GHz)

2.3 RF MEMS CONFIGURATIONS

There are two different areas to an RF MEMS varactor: the actuation (mechanical) section and the electrical section (see Table 1.1) [1]. Electrostatic, magneto static, piezoelectric, or thermal switch designs are used for mechanical movement. To date, switches have been demonstrated at 0.1–100 GHz with high reliability (100 million to 60 billion cycles) and wafer-scale manufacturing techniques. Electrostatic actuation is the most prevalent technique in use today due to its virtually zero power consumption, small electrode size, and thin layers used relatively short switching time (2-24 μ*s*), 50-200 μ*N* of achievable contact forces, and the possibility of biasing the switch using high-resistance bias lines. In many cases, a thermal actuation is coupled with an electrostatic (voltage) hold, or a magneto static actuation (current in a coil) is coupled with a permanent magnetic field.

Table2.2. Different Configuration of MEMS Devices

Actuation Mechanism	Voltage(V)	Current(mA)	Power(mW)	Size	Switching Time	Contact Force(μN)
Electrostatic	20-80	0	0	Small	1-200	50-1000
Thermal	3-5	5-100	0-200	Large	300-10000	500-4000
Magneto static	3-5	20-150	0-100	Medium	300-1000	50-200
Piezoelectric	3-20	0	0	Medium	50-500	50-200

Circuit Configuration	
Series	Shunt
DC-50GHz with metal-to-metal contact and low up-state capacitance 10-50 GHz with capacitive contact and low up state capacitance	DC-60GHz with metal-to-metal contact and low inductance to ground 10-200 GHz with capacitive contact and low inductance to ground
Movements	
Vertical	Lateral
Typically results in small size devices	Typically results in large size devices

2.4. DMTL

DMTL stands for Distributed MEMS Transmission Line Filter .The idea is based on periodically loading transistor, Scotty diodes or passive components such as capacitors or stubs on different types of t-lines to obtain wideband amplifier, oscillators, mixers, filters, multipliers and pulse shaping circuits. Generally DMTL is easier to implement on coplanar waveguide (CPW) line. Line is loaded with shunt switches as variable MEMS capacitors and its number varies with design requirement [1].

For the DMTL, the MEMS capacitors are modeled as a shunt capacitor (C_b) Using this model (L_b and R_{ib} are neglected), the series impedance is $Z_s = j\omega L_t$ and the shunt admittance is $Y_p = j\omega(sC_t + C_b)$ where L_t and C_t are the per unit inductance and capacitance of the unloaded line with impedance Z_0 and are given by

$$C_t = \sqrt{\frac{\varepsilon_{eff}}{cZ_o}} \quad \text{and} \quad L_t = C_t Z_o{}^2 \qquad 2.3$$

where ε_{eff} is the effective dielectric constant of the unloaded t-line and c is the free-space velocity. The characteristic impedance of the loaded line is given by

$$Z = \sqrt{\frac{sL_t}{sC_t + C_b}} \sqrt{1 - \frac{\omega^2}{4} sL_t(sC_t + C_b)} \qquad 2.4$$

So for $C_b = 0$, characteristic impedence equals to Zo, the unloaded impedence of the t-line.

Impedance of loaded line is also given as

$$Z = \sqrt{\frac{sL_t}{sC_t+C_b}}\sqrt{1-\left(\frac{\omega}{\omega_B}\right)^2} \qquad 2.5$$

where $\omega_B$is the Bragg frequency It is a frequency at which the characteristic impedence of line goes to zero i.e. no power transfer.

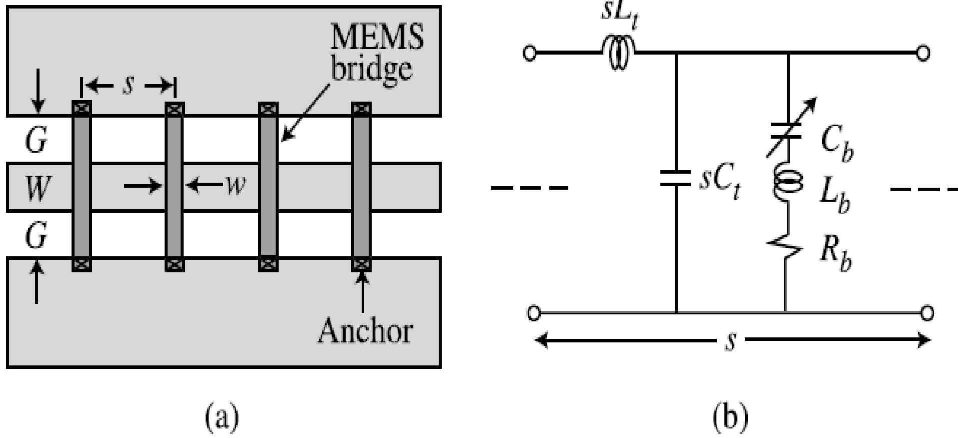

Fig.2.4.(a) DMTL layout (b) Lumped t-line model of single shunt switch section

2.5. RF MEMS TUNABLE BAND-PASS FILTERS

Tracking blocks for multiband telecommunication systems, radiometers, and wide-band radar systems are some of the uses of tunable band-pass filters MEMS filter can greatly simplify the complexity of these systems and reduce the loss. For those applications, filters should to be as flexible as possible in terms of center frequencies and bandwidth. In addition, the tunable band pass filter must be tunable over a wide frequency range with high performance characteristics such as high rejection, ease of integration. Generally, the tunable band-pass filters can be classified into three basic categories: mechanically tunable filters, magnetically tunable filters, and electronically tunable filters. However, none of these satisfies the requirements of miniaturization and mass production. In recent years, tunable band-pass filters based on MEMS technology are being widely studied. It is expected that MEMS technology can bring much improvement to the tradeoffs between tuning range and losses in filter designs. Both the capacitive switch and the metal-contact switch can be used to construct MEMS tunable band-pass filters. The tunable capacitor can be used to construct a tunable band-pass filter. As there are two types of tunable capacitors, the band-pass filter also can be tuned either analogically or digitally [8].

2.5.1 ANALOG TUNING OF A MEMS BAND-PASS FILTER

The metal bridges can be implemented in the structure of the distributed-type band-pass filter to construct a band-pass filter that can be tuned analogically, By lowering the metal bridge without provoking pull-down, the MEMS capacitance changes and hence the electric length of the distribution section are changed. As a result, the center frequency of the band-pass filter is tuned accordingly. A 20 GHz three pole tunable filter based on the distributed transmission-line approach was developed, as shown in Fig. 2.5. The filter demonstrates in insertion loss of 4 to 5 dB and a 3.8-percent tuning range, which is comparably small, as shown in Fig. 2.6.[4]

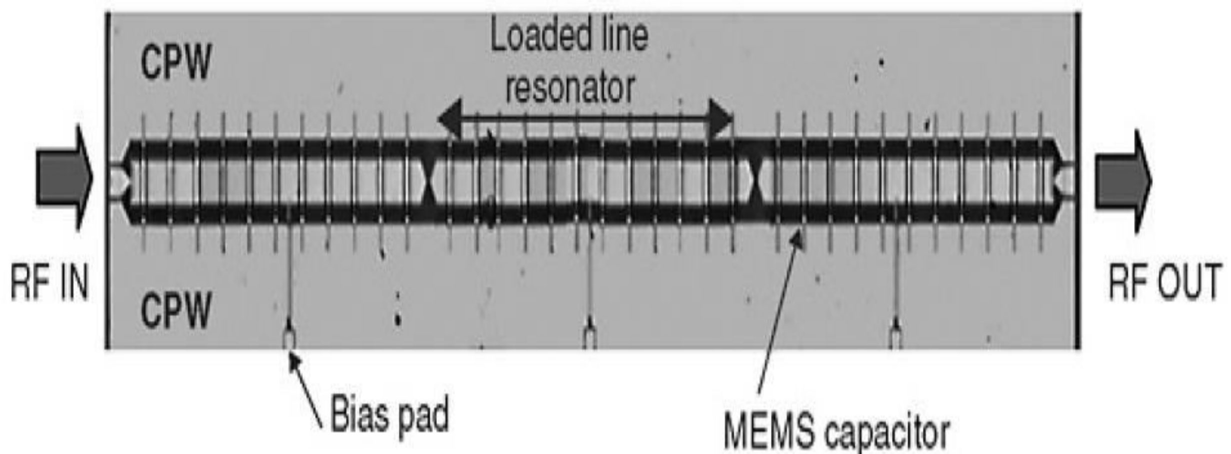

Fig.2.5. Photograph of fabricated three-pole MEMS tunable band-pass filter with distributed MEMS transmission line (DMTL) resonators.

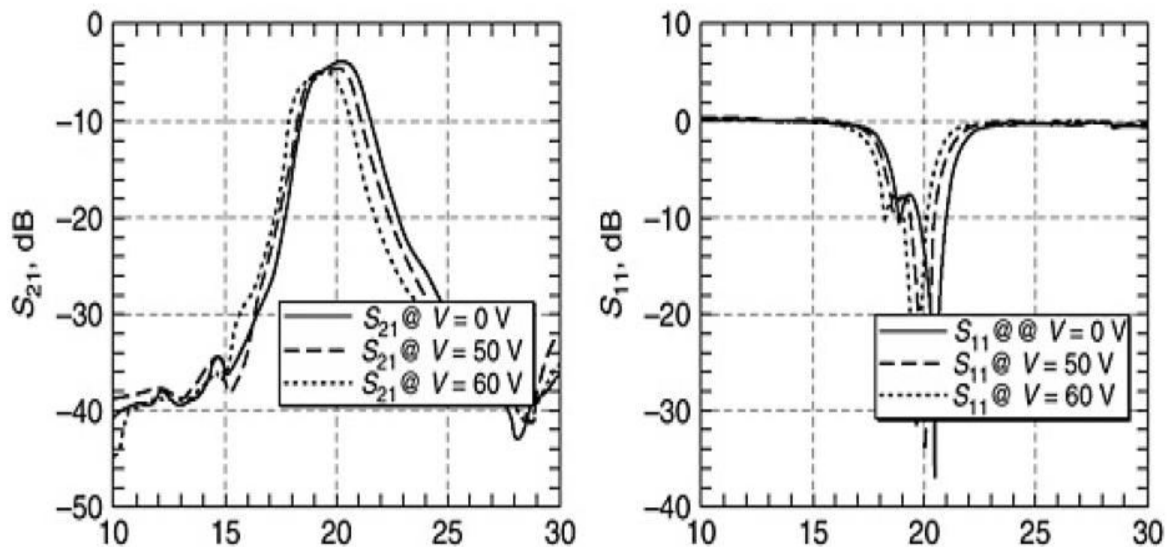

Fig.3.6. Measured S parameters of capacitively coupled MEMS tunable filter

To increase the tuning range and reduce size, another three-pole tunable band-pass filter with 8.6 percent bandwidth based on high-Q MEMS bridge capacitors was designed. The tuning range is 14 percent from 18.6 to 21.4 GHz, with mid band insertion loss of 2.5 dB at 21.1 GHz.[5]

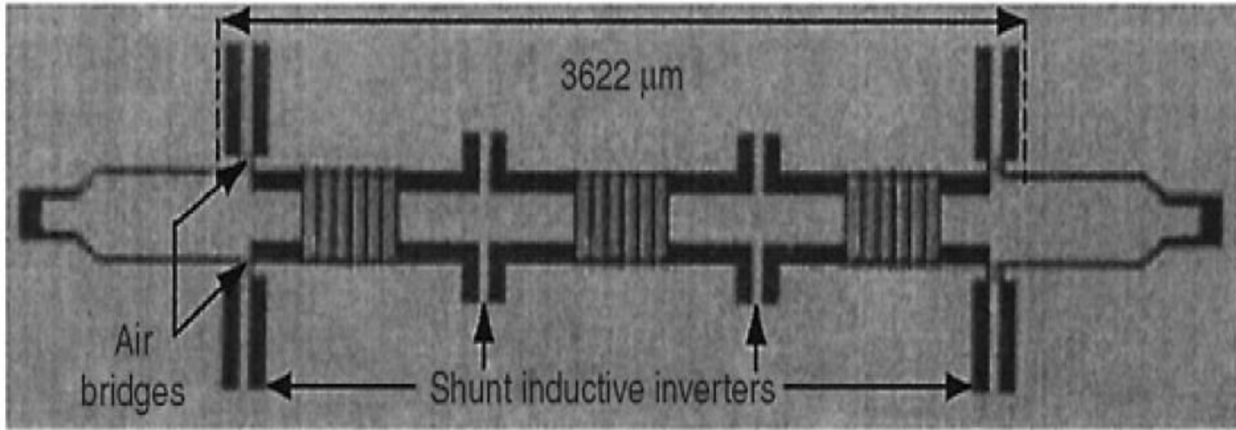

Fig.2.7. Micrograph of the fabricated MEMS miniature filter

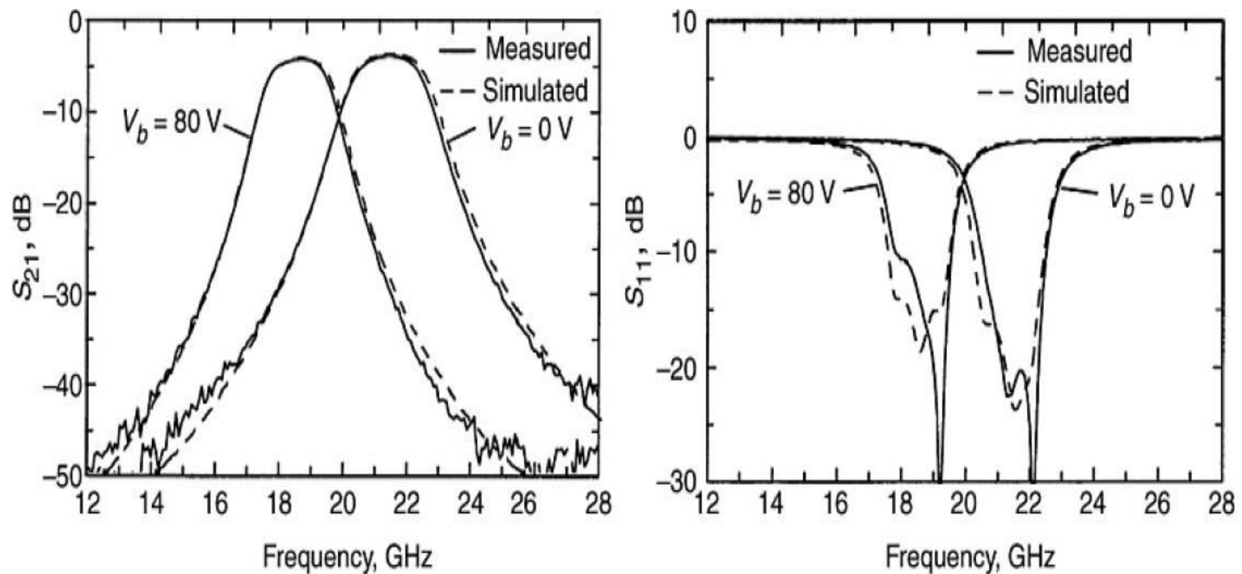

Fig.2.8. Measured and simulated S parameters of the miniature tunable filter for V = 0 and 80 V.

2.5.2 DIGITAL TUNING OF AN RF MEMS FILTER

In such band-pass filter, the capacitive switches are used digitally and therefore change the capacitance values of the structure. In such designs, series resonators are converted to shunt parallel resonators using impedance inverters first, and then both the series and shunt capacitors are tuned by the capacitive switches, as shown in Fig. 2.9.[6]

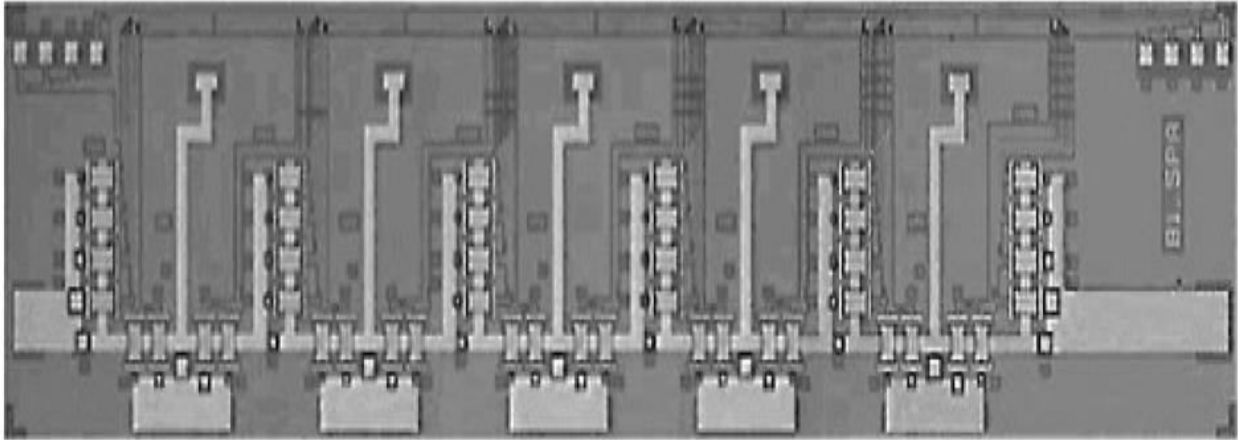

Fig. 2.9. Layout of the UHF five-pole filter

In this design, the key is the wide selection of capacitance values and capacitance steps that can be achieved with a 4-bit MEMS switched capacitor. The measurement results are given in Fig. 43.10, which shows an insertion loss of between –6.6 and –7.3 dB along with a reflection coefficient that is better than –10 dB for all 16 tuning steps.

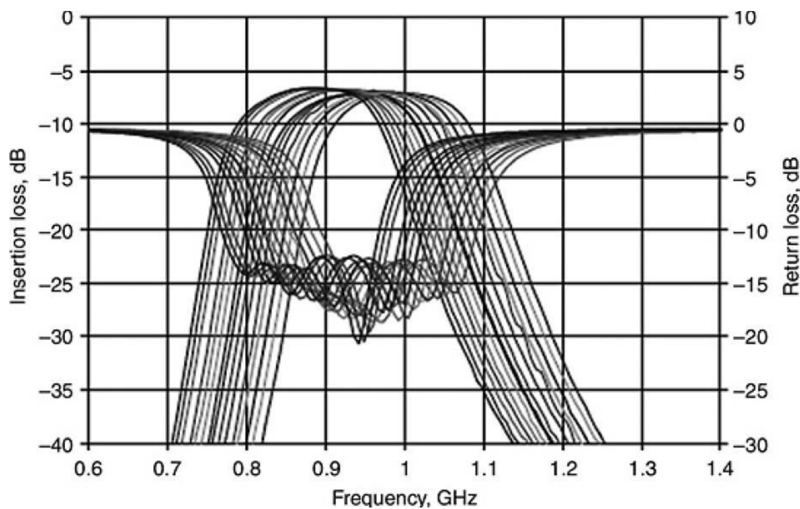

Fig. 2.10. UHF responses

CHAPTER 3
MICROWAVE FILTER THEORY

3.1 INTRODUCTION

Microwave filter is a two port network to control the transmission of frequencies in pass band range and attenuation in stop band range. Typically there are four types of filters low pass, high pass, band pass and band reject . They are having frequent applications in microwave communication, radar, or test and measurement systems.

There are so many method of filter design like periodic structures, image parameter method and insertion loss method but these methods provide lumped element circuit which is modified to distributed elements using Richard transformation and Kuroda identities. Apart from these, stepped impedance, coupled line and filter using coupled resonator are the most frequent methods.

Today most of the design is based on Insertion loss method using CAD tools because of continuous advancements in network synthesis with distributed element and its compatibility with active devices in filter circuits. This chapter is mainly focused on design of band pass filter with insertion loss method and filter using coupled resonator method and these topics are discussed in detail[7] .

3.2 FILTER DESIGN METHODS

3.2.1 PERIODIC STRUCTURE

It consist of transmission line periodically loaded with reactive elements such structures are the subject of interest because of its application in slow wave structure and travelling wave amplifier design. It exhibits basic pass band response that leads to image parameter method of design.

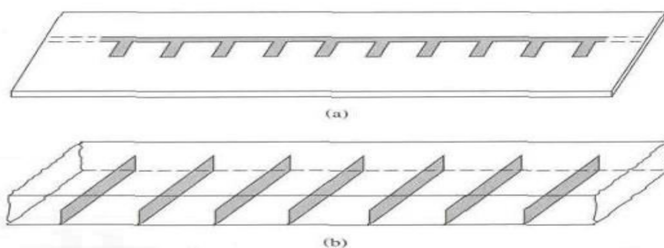

Fig.3.1. (a) Periodic stub on microstrip line (b) Periodic diaphragm in waveguide

3.2.2 IMAGE PARAMETER METHOD

It consists of cascade of simple two port filter section to provide the desired cutoff and attenuation characteristics, but do not allow the specification of a frequency response over the complete operating range. This method is simple but design is often iterated many times to achieve desired result.

Similar concept of iteration has been used in this project to improve the attenuation characteristics.

3.2.3 INSERTION LOSS METHOD

It is a technique to design filters with a completely specified frequency response. It begins with low pass filter prototype design that is normalized in terms of impedance and frequency. Then transformations are applied to convert the prototype to desired frequency range and impedance level. After that design is modified to distributed elements using Richard's transformation and Kurodo identities for practical implementation.

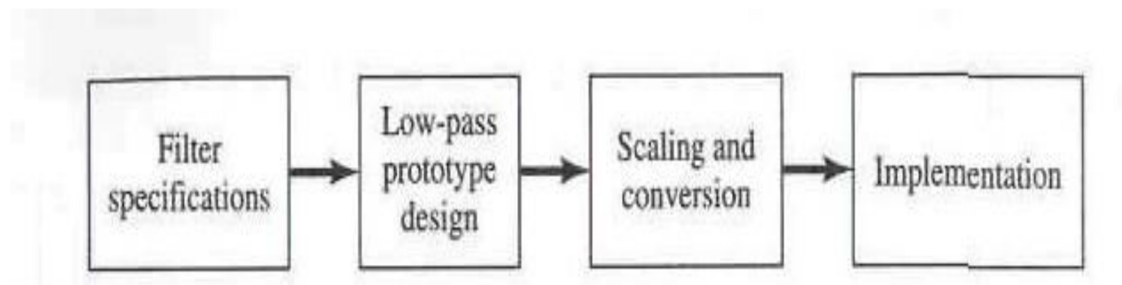

Fig. 3.2.The process of filter design by insertion loss method

LOW PASS PROTOTYPE DESIGN

While designing the low pass prototype, most important thing is to choose the binomial response. Among them, Chebyshev and maximally flat are the responses that are mainly used. Chebyshev response satisfies a requirement for sharpest cutoff .on other hand Maximally flat also called binomial or Butterworth response is optimum in sense that it provides the flattest possible pass band response for a given filter complexity or order.

There are some graphical relations and tables reproduced from the book "Microwave Engineering" by Pozar based on which the order of the filter is decided.

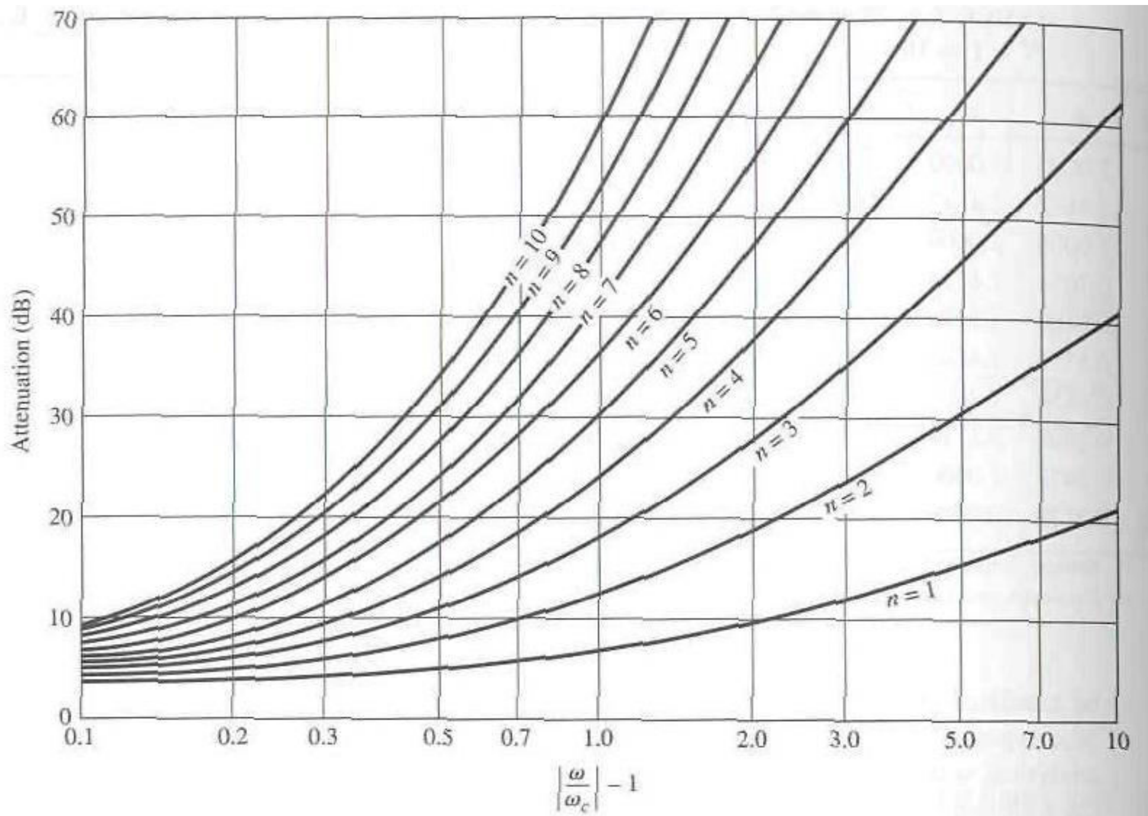

Fig. 3.3.Attenuation verses normalized frequency for maximally flat filter prototype

Table3.1. Elemental values for maximally flat low pass filter prototype (g_o=1, c_o=1, N=1 to 10)

N	g1	g2	g3	g4	g5	g6	g7	g8	g9	g10	g11
1	2.0000	1.0000									
2	1.4142	1.4142	1.0000								
3	1.0000	2.0000	1.0000	1.0000							
4	0.7654	1.8478	1.8478	0.7654	1.0000						
5	0.6180	1.6180	2.0000	1.6180	0.6180	1.0000					
6	0.5176	1.4142	1.9318	1.9318	1.4142	0.5176	1.0000				
7	0.4450	1.2470	1.8019	2.0000	1.8019	1.2470	0.4450	1.0000			
8	0.3902	1.1111	1.6629	1.9615	1.9615	1.6629	1.1111	0.3902	1.0000		
9	0.3473	1.0000	1.5321	1.8794	2.0000	1.8794	1.5321	1.0000	0.3473	1.0000	
10	0.3129	0.9080	1.4142	1.7820	1.9754	1.9754	1.7820	1.4142	0.9080	0.3129	1.0000

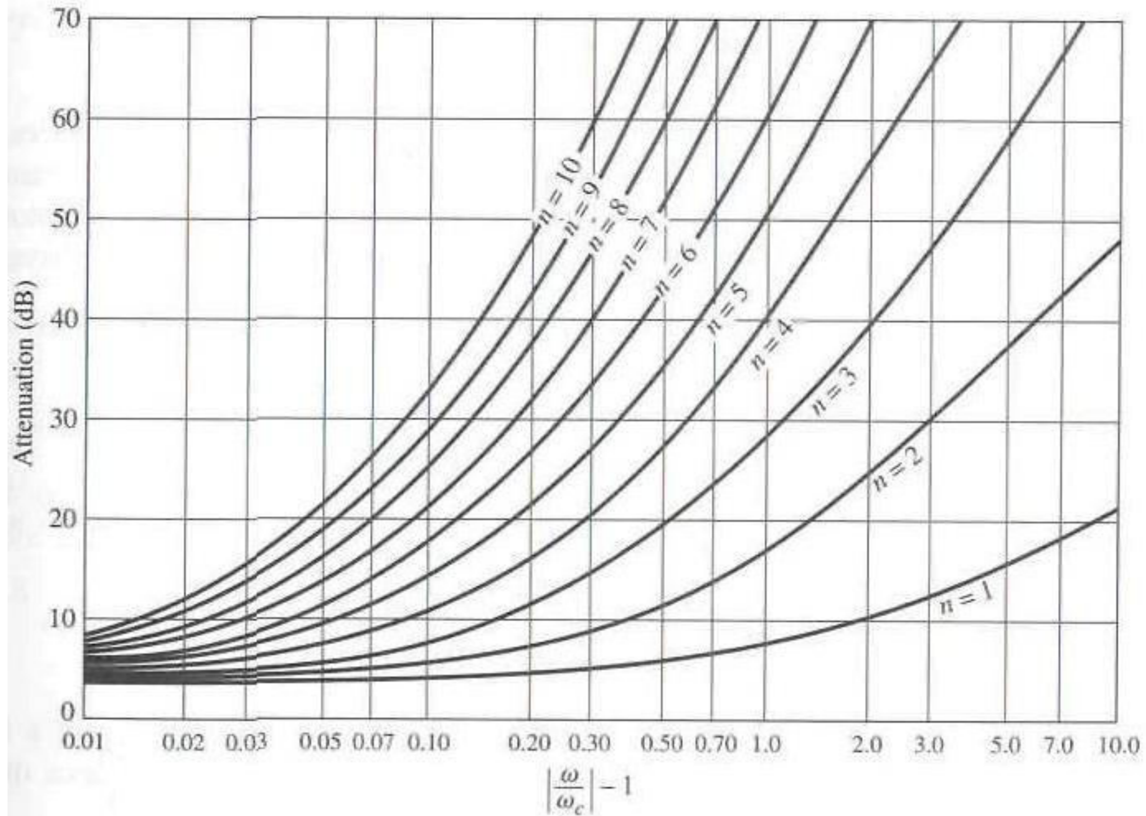

Fig. 3.4 .Attenuation verses normalized frequency for Equal ripple filter prototype

Table3.2.Elemental values for maximally flat low pass filter prototype (g_o=1, c_o=1, N=1 to 10)

N	g1	g2	g3	g4	g5	g6	g7	g8	g9	g10	g11
1	1.9953	1.0000									
2	3.1013	0.5339	5.8095								
3	3.3487	0.7117	3.3487	1.0000							
4	3.4389	0.7483	4.3471	0.5920	5.8095						
5	3.4817	0.7618	4.5381	0.7618	3.4817	1.0000					
6	3.5045	0.7685	4.6061	0.7929	4.4641	0.6033	5.8095				
7	3.5182	0.7723	4.6386	0.8039	4.6386	0.7723	3.5182	1.0000			
8	3.5277	0.7745	4.6575	0.8089	4.6990	0.8018	4.4990	0.6073	5.8095		
9	3.5340	0.7760	4.6692	0.8118	4.7272	0.8118	4.6692	0.7760	3.5340	1.0000	
10	3.5384	0.7771	4.6768	0.8136	4.7425	0.8164	4.7260	0.8051	4.5142	0.6091	5.8095

where,

- g_o is defined as the source resistance/conductance.

- g_1 for i = 1 to N represent either the inductance of a series inductor or the capacitance of a shunt capacitor, therefore n is also the number of reactive elements.
- g_{N+1} is the load resistance/conductance.
- The g-values are the inductance in Henry (H), capacitance in farad (F), resistance in ohm (Ω) and conductance in Siemens (S) or mhos.

So, as specification if it's given that cutoff frequency is 8 GHz and 20dB attenuation is needed at 11 GHz then from

$$\left|\frac{\omega}{\omega_c}\right| - 1 = \left|\frac{11}{8}\right| - 1 = 0.375 \qquad 3.1$$

Using above graph, we can know the order of filter for given attenuation. For that corresponding N value, we can get elemental values form the table. So the ladder like circuit becomes like

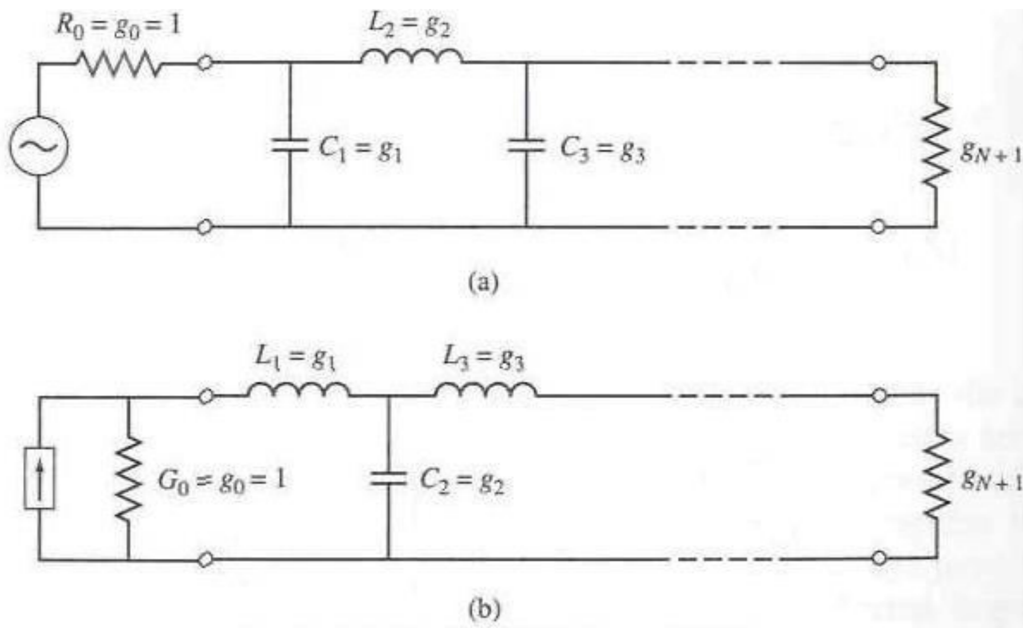

Fig. 3.5.(a) Prototype begins with a shunt element (b) Prototype begins with a series element

IMPEDANCE SCALING

In prototype design, the source and load resistances are unity .A source resistance R_o can be obtained by multiplying the impedance of prototype design by R_o. So the component value becomes

$$L' = R_o L \quad 3.2$$

$$C' = \frac{C}{R_o} \quad 3.3$$

$$R'_S = R_o \quad 3.4$$

$$R'_L = R_o R_L \quad 3.5$$

where L, C, R_L are component values for the original prototype

FREQUENCY SCALING

To change the cut off frequency from unity to ω_c, we need to scale the frequency by factor $1/\omega_c$ And the component values becomes

$$L' = {R_o L}/{\omega_c}$$

3.6

$$C' = C/(Ro\ \omega_c) \quad 3.7$$

BAND PASS TRANSFORMATION

Low pass prototype design can be transformed to have band pass response. If ω1 and ω2 denotes the edge of pass band then BPF behavior can be obtained using frequency substitution

$$\omega \leftarrow \frac{\omega_o}{\omega_2-\omega_1}\left(\frac{\omega}{\omega_o} - \frac{\omega_o}{\omega}\right) = \frac{1}{\Delta}\left(\frac{\omega}{\omega_o} - \frac{\omega_o}{\omega}\right) \quad 3.8$$

where $\Delta = \frac{\omega_2-\omega_1}{\omega_o}$ is the fractional bandwidth for the pass band.

The central frequency ω_o could be chosen as the arithmetic mean of ω_2 and ω_1 or sometimes as geometrical mean. So series inductor L_k is transformed to series LC circuit with element values

$$L'_k = \frac{L_k}{\Delta\omega_o} \quad 3.9$$

$$C'_k = \frac{\Delta}{\omega_o L_k} \quad 3.10$$

And shunt capacitor C_k is transformed to shunt LC circuit with element values

$$L'_k = \frac{\Delta}{\omega_o C_k} \qquad 3.11$$

$$C'_k = \frac{C_k}{\Delta \omega_o} \qquad 3.12$$

So circuit becomes like

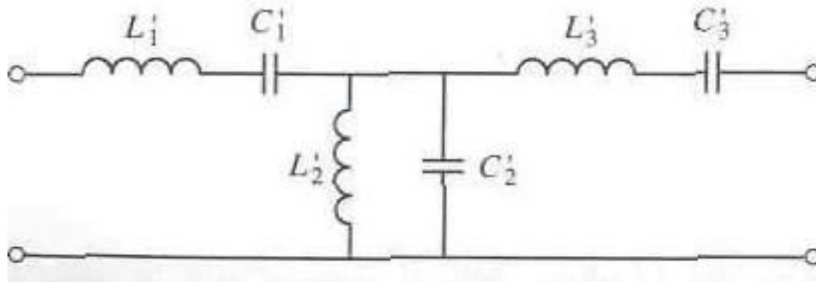

Fig. 3.6.Band pass circuit

3.2.4 STEPPED IMPEDANCE METHOD

It's a way to implement low pass filter by using alternating sections of very high and very low characteristic impedance lines. It is popular because it is easier to design and takes less space. But its electrical performance is not good so has limited application

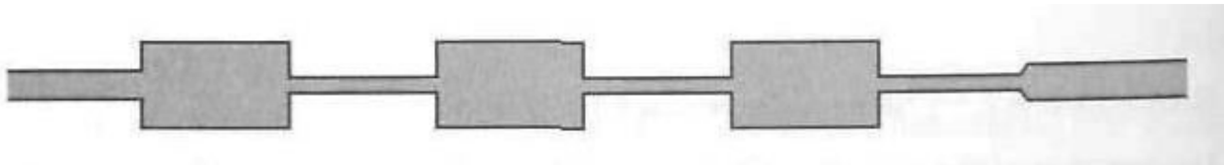

Fig. 3.7. Microstrip layout of stepped impedance filter

3.2.5 COUPLED LINE FILTER

Fabrication of multi section band pass or band stop coupled line filter is easy to design for band width less than 20%. Wider bandwidth filters are difficult to design as coupled lines are closely spaced which is difficult to fabricate.

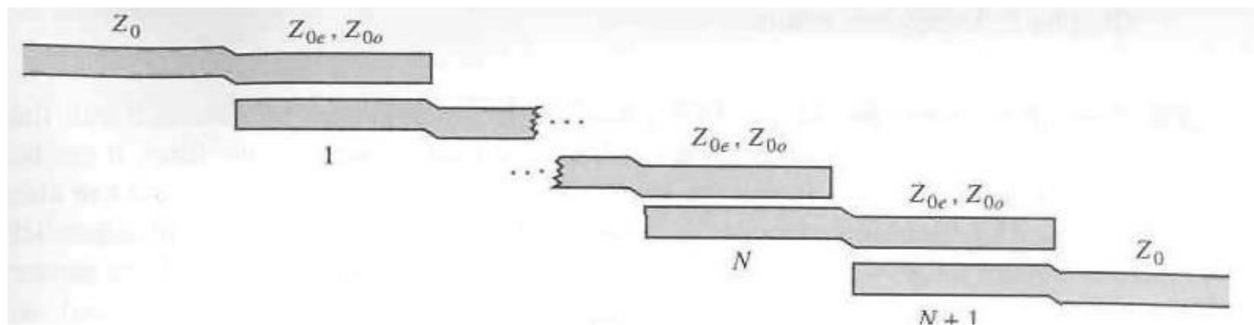

Fig. 3.8. Layout of coupled line filter

3.2.6 BAND PASS FILTER USING CAPACITIVELY COUPLED RESONATORS

Band pass filter can be conveniently fabricated in Microstrip and Coplanar waveguide line using this method. An Nth order filter will have N resonator section and N+1 capacitive gap between them. The resonator length is approximately $\frac{\lambda}{2}$ long at the central frequency. To find the electrical length (θ) and series capacitance (C_n) following design equations are used

$$Z_o J_1 = \sqrt{\frac{\pi\Delta}{2g_1}} \qquad 3.13$$

$$Z_o J_n = \frac{\pi\Delta}{2\sqrt{g_{n-1} - g_n}} \qquad 3.14$$

$$Z_0 J_{n+1} = \sqrt{\frac{\pi\Delta}{2g_N g_{N+1}}} \qquad 3.15$$

where Z_0 is characterics constant and J_i is the admittance inverter constant

Resulting inverter constant can be related to capacitive susceptance as

$$B_i = \frac{J_i}{1-(Z_o J_i)^2} \qquad 3.16$$

And coupling capacitance value as

$$C_n = \frac{B_n}{\omega_n} \qquad 3.17$$

Finally the electrical length of resonator section can be found as

$$\theta_i = \pi - \frac{1}{2}[\tan^{-1}(2Z_o B_i) + \tan^{-1}(Z_o B_{i+1})] \qquad 3.18$$

This method has been used as a basis for filter design in this thesis.

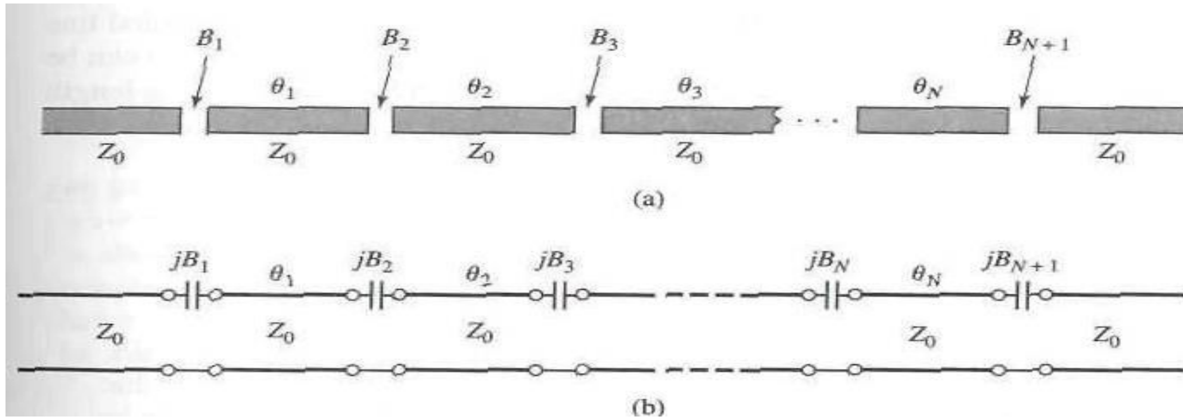

Fig. 3.9.(a) Capacitive gap coupled resonator band pass filter (b) Transmission line model

CHAPTER 4

ELECTROMAGNETIC MODELING AND DESIGNING OF THE FILTER

4.1 INTRODUCTION

This chapter details the basic design strategies and electromagnetic modeling of the unit cell structure and single pole capacitively coupled DMTL section of the designed filter. The unit cell is nothing but one of several MEMS miniaturized capacitive shunt switches loaded on a CPW line. Depending on the applied DC bias voltage to central signal line, the membrane or beam of shunt capacitive switch is actuated which results in variable resonator length.

4.2. ELECTROMAGNETIC MODEL OF THE MEMS CAPACITOR

The cross-sectional view of the unit cell structure has been shown in Fig.4.3. A 60/100/60µm 50Ω CPW line of 1µm thick gold has been made on 270µm thick silicon substrate and the MEMS capacitor is designed using shunt switch. A beam of 2µm thick and 300µm long is fixed on both sides by means of anchors and the anchors are connected to the two ground planes of the CPW line. Both the anchors and the bridge are made of gold. A 0.2µm thick layer of silicon nitride (Si_3N_4) on top of the central conductor acts as a dielectric to ensure capacitive contact between the bridge and the signal line of the CPW. The air gap between the beam and the signal line is g_0=3µm above nitride layer.

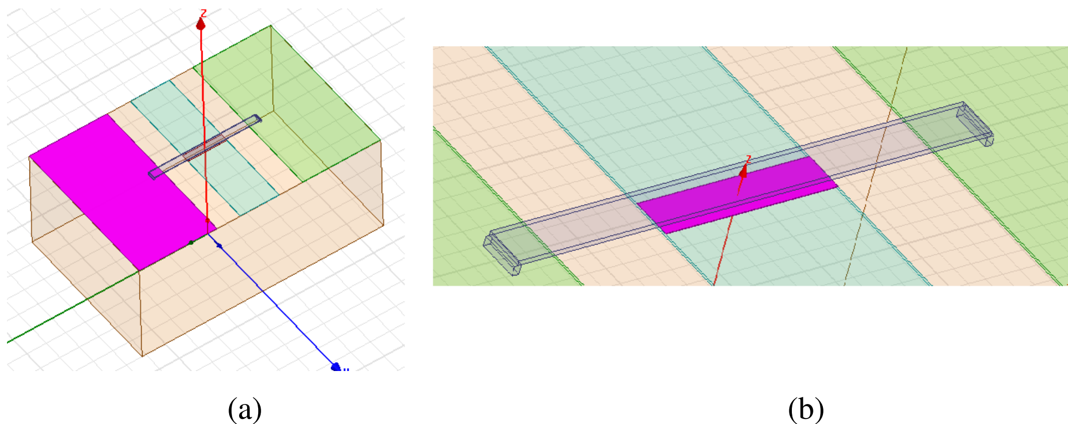

(a) (b)

Fig.4.1. The cross sectional view of the MEMS capacitor

It is to be noted that, a single fixed-fixed beam shunt switch can be equivalently modeled by a series RLC circuit placed in shunt with a transmission line section as shown in Fig. 4.2

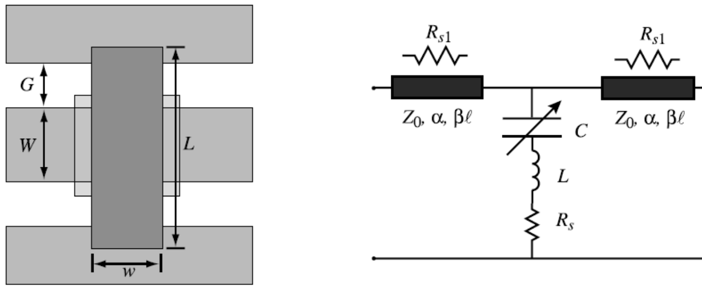

Fig. 4.2: Equivalent CLR model of the capacitive switch

The switch shunt impedance is given by

$$Z_S = R_S + j\omega L + \frac{1}{j\omega C} \qquad 4.1$$

where C=C_u or C_d depending on the position on the switch. The LC series resonant frequency of the shunt bridge is

$$f_O = \frac{1}{2\pi\sqrt{LC}} \qquad 4.2$$

And the impedance of the shunt bridge can be approximated by

$$Z_S = \begin{cases} \frac{1}{j\omega C} & for \;\; f \ll f_O \\ R_S & for \;\; f = f_O \\ j\omega L & for \; f \gg f_O \end{cases} \qquad 4.3$$

The CLR model behaves as a capacitor below the LC series resonant frequency and as an inductor above the frequency. At resonance, the CLR model reduces to the series resistance of the MEMS capacitor.

The capacitance and inductance of the designed MEMS capacitor have been obtained using Maxwell 3D and HFSS software respectively. From Table 4.1 and Table 4.2 resonance frequency can be calculated and is much higher than 15GHz. So, inductance and resistance plays absolutely no role for frequency around 15GHz for bridge position for air gap from g_o= 2 μm to 3 μm but the inductance becomes dominant in the down state position. But we are not concerned with down state position for this project. Therefore, the designed shunt switch can be accurately

modeled as a shunt capacitance to ground.

Table4.1. MEMS capacitance variation with air gap

Air gap (µm)	Capacitance (fF) C_{MEMS}
g= 0	99.928
g= 2	11.171
g= 2.5	9.509
g= 3	8.313

Table4.2. MEMS Inductance variation with air gap

Air gap (µm)	Inductance (pH)
g= 2	6.174
g= 2.5	6.046
g= 3	7.64

Fig.4.3 (a) and (b) shows the electrostatic actuation mechanism of operation of a capacitive shunt switch. Fig.3.5 (a) represents the up-state when no actuation voltage has been applied whereas Fig.3.5(b) represents the actuated -state when biasing is applied.

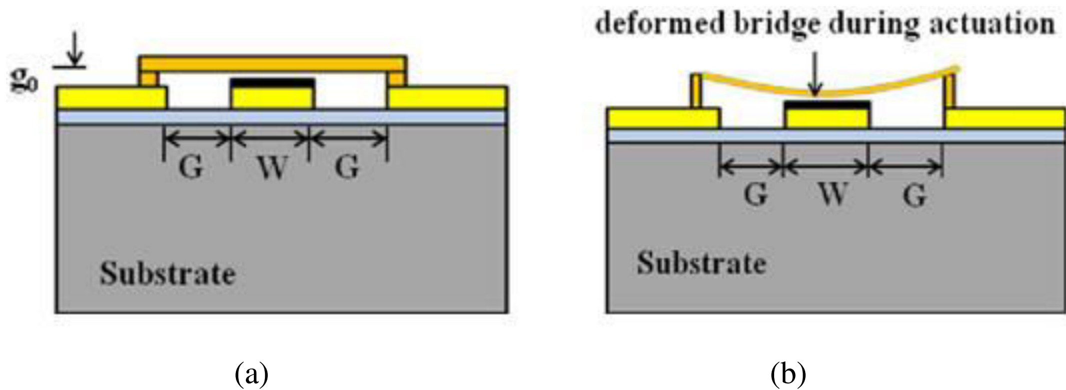

(a) (b)

Fig.4.3. (a) MEMS capacitive shunt switch in up-state, (b) MEMS capacitive shunt switch in actuated-state

The parallel plate capacitance of the MEMS capacitor can given as

$$C = C_{PP} + C_f \qquad 4.4$$

$$C_{pp} = \frac{\varepsilon_O w W}{g_O + \frac{t_d}{\varepsilon_{rd}}} \qquad 4.5$$

where

t_d =thickness of the dielectric

A=capacitive area of the bridge (W x w)

ε_O =permittivity of free space

ε_{rd} =permittivity of dielectric

g_0=air gap in unbiased state

C_f = fringing capacitance

Table4.3. Simulated Static capacitance of the designed MEMS capacitor (L=300 µm, bridge thickness=2 µm, t_d= 0.2 µm, $\varepsilon_{rd} = 7.5$, w x W = 20 x 100 µm^2)

g_o (µm)	C[fF]	C_{PP}[fF]	C_f [fF]	C_f / C_{PP}
1	18.450	17.20	1.25	7.26%
1.5	13.869	11.59	2.779	23.98%
2	11.171	8.73	2.441	27.96%
2.5	9.509	7.00	2.509	35.84%
3	8.313	5.85	2.463	42.10%
3.5	7.487	5.02	2.467	49.14%

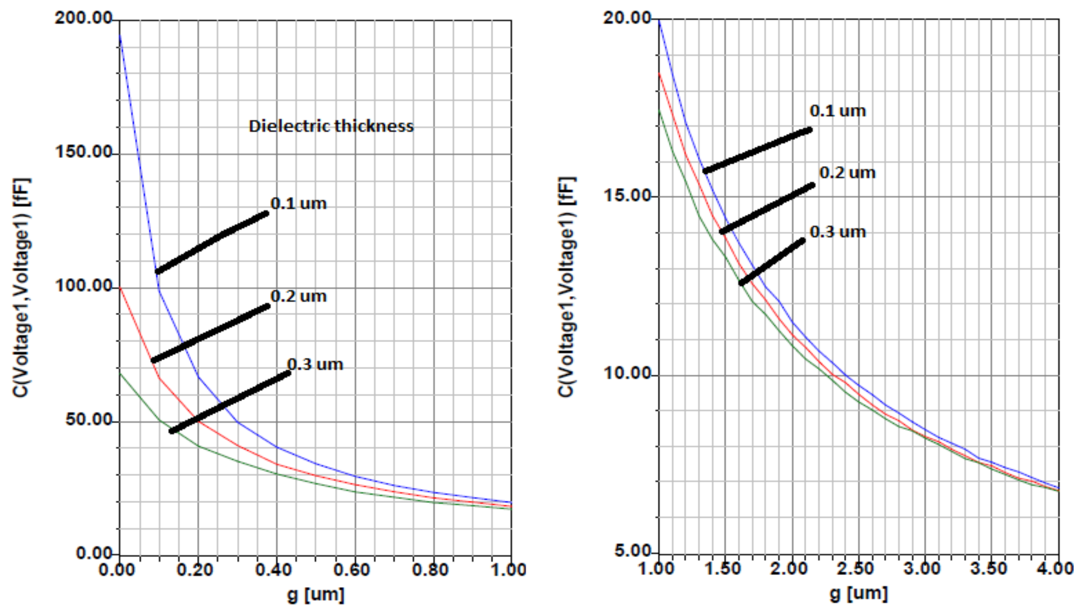

Fig.4.4. Simulated result of Capacitance verses air gap between central line and Shunt Bridge (L=300 µm, bridge thickness=2 µm, t_d= 0.2 µm, $\varepsilon_{rd} = 7.5$, w x W = 20 x 100 µm^2)

Variation of capacitance with change in air gap and thickness of nitride layer has been shown in Fig.4.4. Difference between total capacitance and the parallel plate capacitance indicate that the fringing capacitance is substantial portion of MEMS capacitance (Table 4.3). It is reported that fringing capacitance is around 20% to 60% of the parallel plate capacitance, depending upon bridge dimension and height. Therefore fringing capacitance cannot be neglected in the analysis.

4.3. ANALYTICALLY CALCULATED MODEL PARAMETERS FOR DMTL SECTION

When the unit structures as shown in previous section are cascaded, it results in DMTL section. and its equivalent circuit can be shown as Fig. 4.5

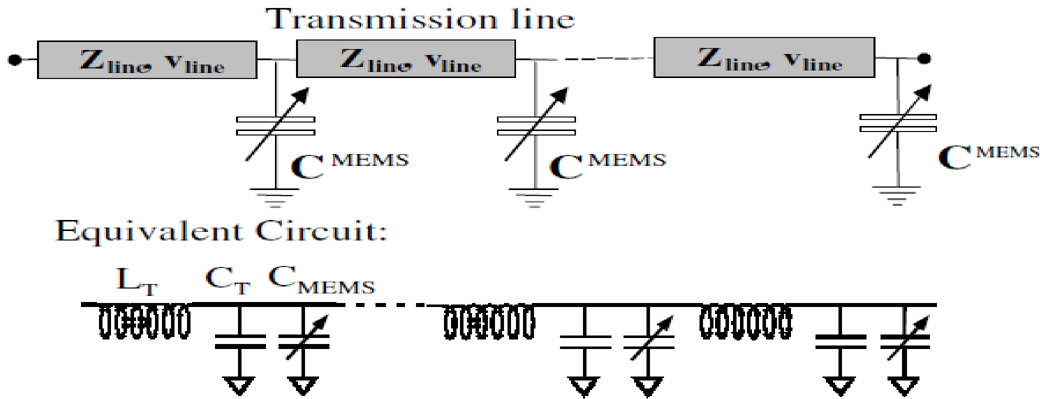

Fig.4.5. Schematic and equivalent circuit of a DMTL

where L_t : Transmission line inductance per section

C_t : Transmission line capacitance per section

s : Length of transmission line per section

The values of inductance L_t and capacitance C_t of the DMTL can be found as per equation 2.3. For the design, C_t and L_t are found to be 2.074 x 10^{-5} F and 5.185 x 10^{2} H respectively. The effective permittivity is given as

$$\varepsilon_{eff} = \frac{1+\varepsilon_{eff}}{2} \quad 4.6$$

It is 6.45, considering ε_r for silicon is 11.9. Characteristic impedance of loaded line is given as per equation 2.4 and is almost 50 Ω for go from 2 µm to 3 µm since C_{MEMS} is negligible with respect to C_t.

4.4. DESIGN OF SINGLE POLE BAND PASS FILTER

To make the band pass filter using capacitively coupled resonator technique, the DMTL section is to be approximately one-half wavelength long at pass band frequency and the coupling capacitor are chosen to give the correct bandwidth. A single pole resonator topology has been used as shown in Fig.4.6.

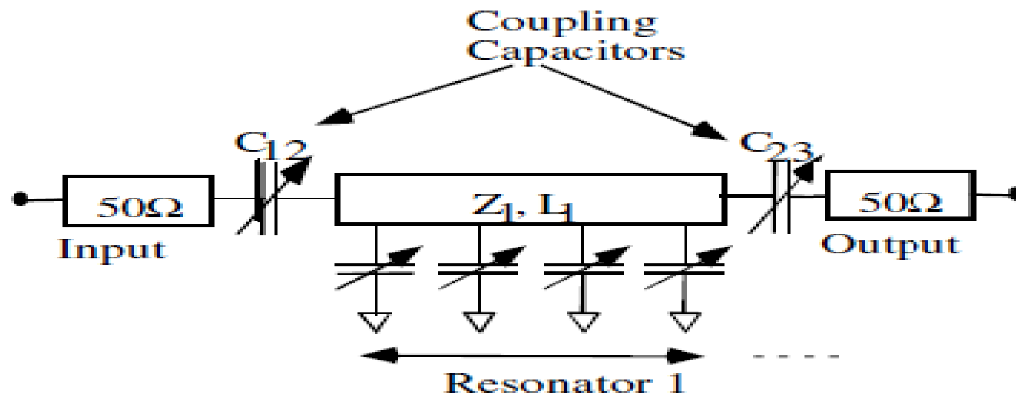

(a)

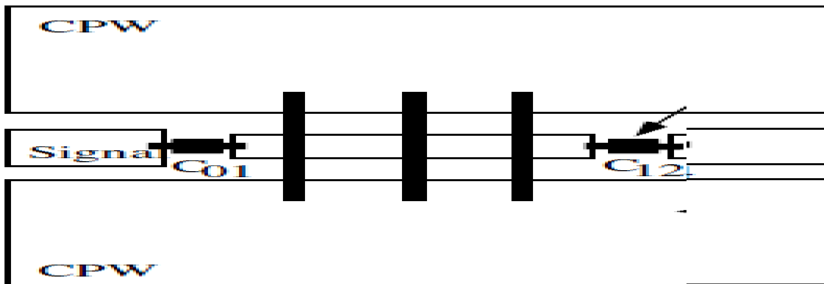

(b)

Fig.4.6. (a) Topology of single pole capacitively coupled resonators. (b) Layout tunable filter in coplanar-waveguide form

So, Aligent ADS line cal tool has been used to yield the required G/W/G dimension corresponding to 50Ω impedance. Obtained 60/100/60µm CPW with 12 MEMS capacitors are designed in HFSS v13 software. The number of Bridge sections in a resonator is calculated as per following relation

$$n = \frac{f_{Bragg}}{f_o}\frac{l_{elec}\pi}{360} \qquad 4.7$$

where f_{Bragg} is a chosen Bragg frequency which is chosen to be almost 8 to 10 times of central

frequency. l_{elec} is approximately taken as half of the required wavelength. Coupling capacitors has been realized using three parallel down state cantilever switch like structure in the dissertation work as shown in Fig. 4.8.

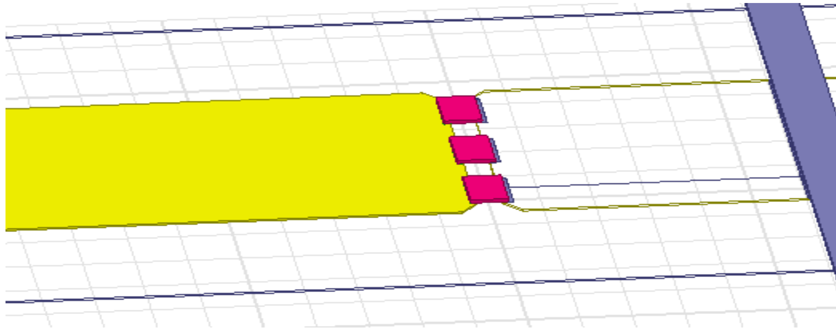

Fig. 4.9.Coupling capacitors

The whole single pole structure has been cascaded and parametric tuning has been carried out on HFSS to trade off between losses, bandwidth and band rejection. As per design equation 3.13 to 3.18 , the coupling capacitances and electrical length of resonator at 15.2 GHz has been shown in Table 4.4

Table 4.4.Summary of $C_{i-1,i}$ and l_{elec}

i	$C_{i-1,i}$ [fF]	$l_{elec\ i}$
1	98.68	136.7
2	98.68	

CHAPTER 5
ELECTROMECHANICAL MODELING OF THE FILTER

5.1 INTRODUCTION

This chapter details the electromechanical modeling of the proposed unit cell structure under electrostatic forces. Here, the value of voltage required to actuate the fixed-fixed beam of capacitive shunt switch has been computed. The electromechanical simulation part has been carried out by means with the aid of software Coventor MEMS+.

5.2 STATIC ANALYSIS

Static Analysis refers to the curve or plot of displacement against actuation voltage. In this design, DC bias voltage is given to the central signal line of each resonator section. So, most of the discussion has been done for fixed-fixed beam when the force is evenly distributed over the central portion (Fig.5.1).

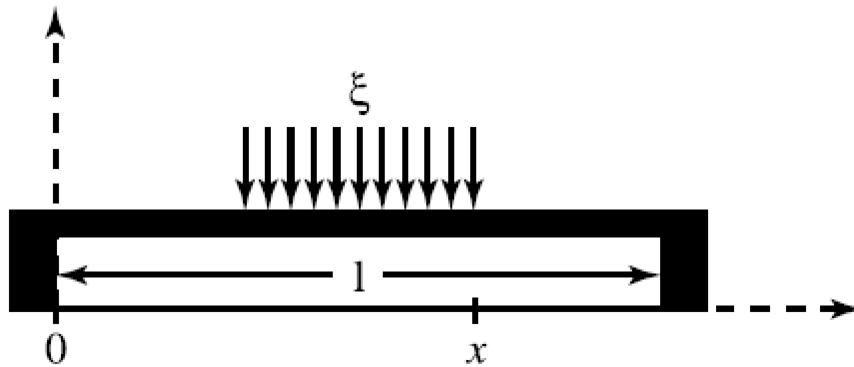

Fig. 5.1.Fixed–fixed beam with the force, evenly distributed about the center of the beam.

5.2.1 SPRING CONSTANT OF FIXED –FIXED BEAM SHUNT SWITCH

The mechanical actuation depends on its spring constant of the beam. If the operation of the of the structure is limited to small deflection, as in the case for most RF MEMS devices, the mechanical behavior can be modeled using a linear spring constant, k (N/m). The deflection, Δg

(m), of the fixed-fixed beam for an external force, F (N), can then be obtained using F= k*Δg. Fixed-fixed beams are commonly used due to their relatively high spring constant and ease of manufacturing. The spring constant for the fixed-fixed beam can be modeled in two parts. One part, k′, is due to the stiffness of the bridge which accounts for the mechanical characteristics such as Young’s modulus, E (Pa), and the moment of inertia, I (m^4). The other part of the spring constant, k″, is due to the biaxial residual stress, (Pa) within the beam and is a result of fabrication process.

For a beam over a CPW line with the center conductor width being a third of the length of beam with force distributed above the center conductor, the total spring constant is found to be

$$k = k_c' + k_c'' \tag{5.1}$$

Spring Constant Due to Beam Stiffness

$$k_c' = 32Ew\left(\frac{t}{l}\right)^3\left(\frac{27}{49}\right)N/m \tag{5.2}$$

Spring Constant Component Due to Residual Stress

$$k_c'' = 8\sigma(1-v)w\left(\frac{t}{l}\right)\left(\frac{3}{5}\right)N/m \tag{5.3}$$

where

t : thickness of beam

l : length of beam

v : Poisson’s ratio (0.42 to 0.44)

E: Young’s modulus (Pa)[80GPa for gold]

w : width of beam

σ : residual stress

For the gold beam of 20μm wide and 2μm thick, Fig.5.2.(a), (b) and (c) shows the variation of (k_c') spring constant due to beam stiffness, variation of (k_c'') spring constant component due to residual stress and total spring constant respectively with t/l ratio and a residual stress of 30MPa and 60MPa. Poisson’s ratio is taken to be 0.43. [10]

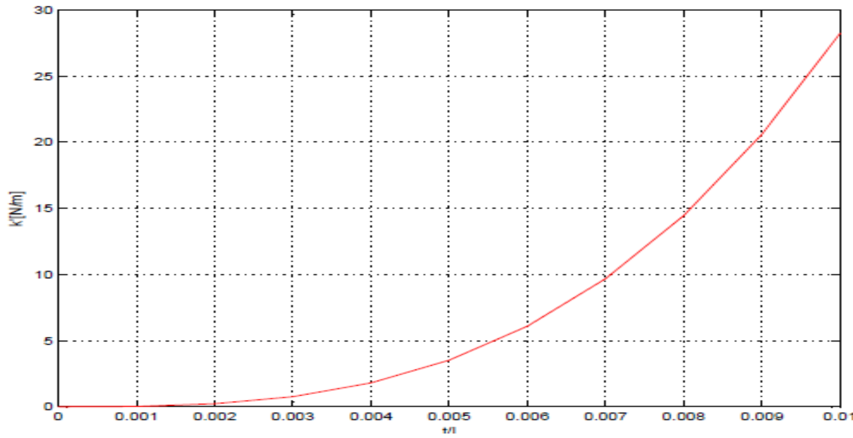

Fig. 5.2.(a) Spring Constant Due to Beam Stiffness

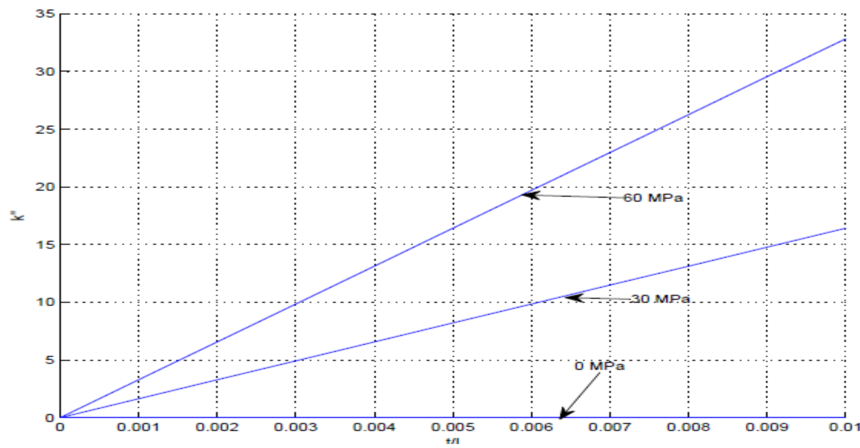

Fig. 5.2.(b) Spring Constant Due to residual stress

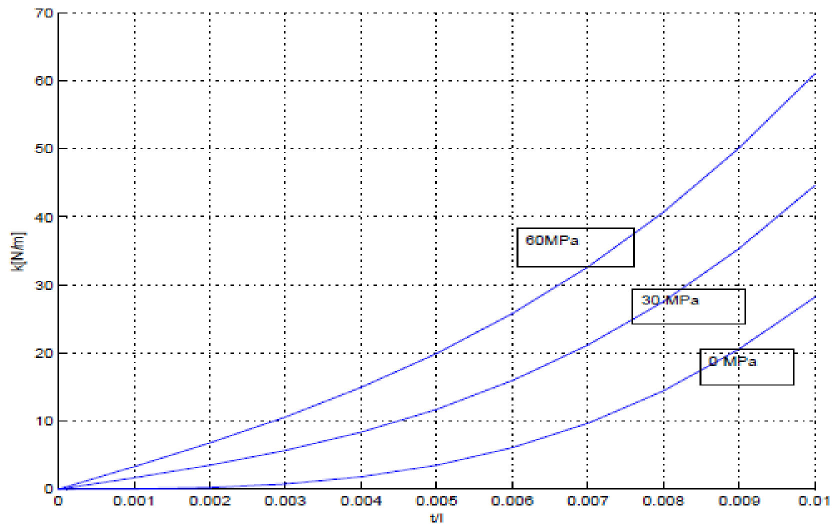

Fig. 5.2.(c) Total spring constant

For the designed capacitive beam, spring constant has been surmised in Table5.1

Table5.1. Summary of spring constant for 20 µm x 300 µm fixed-fixed beam

$\sigma[MPa]$	k_c'[N/m]	k_c'' [N/m]	$k[N/m]$
0	8.3592	0	8.3592
30	8.3592	10.944	19.3032
60	8.3592	21.888	30.2472

5.2.2 ELECTROSTATIC ACTUATION ANALYSIS

When DC bias is applied across central signal line and the shunt switches, an electrostatic force is induced on the beams. Although; the actual capacitance is about 20-40% larger due to fringing fields. In order to approximate this force; the beam over the pull-down electrode is modeled as a parallel-plate capacitor.

For given (w) width of beam, (W) width of electrode, (g) height of beam when actuated due to induced force and (go) beam height in unbiased state, the relation between actuation and voltage applied is given as

$$V = \sqrt{\frac{2k}{wW\epsilon_O} g^2(go - g)} \qquad 5.4$$

where V is the voltage applied between the beam and the electrode. Equation (5.4) neglects the effect of the dielectric layer between the bridge and the pull-down electrode. Fig.5.3 shows the plot of the beam height verses applied voltage for the designed MEMS capacitor. It shows two possible beam positions for every applied voltage.[10]

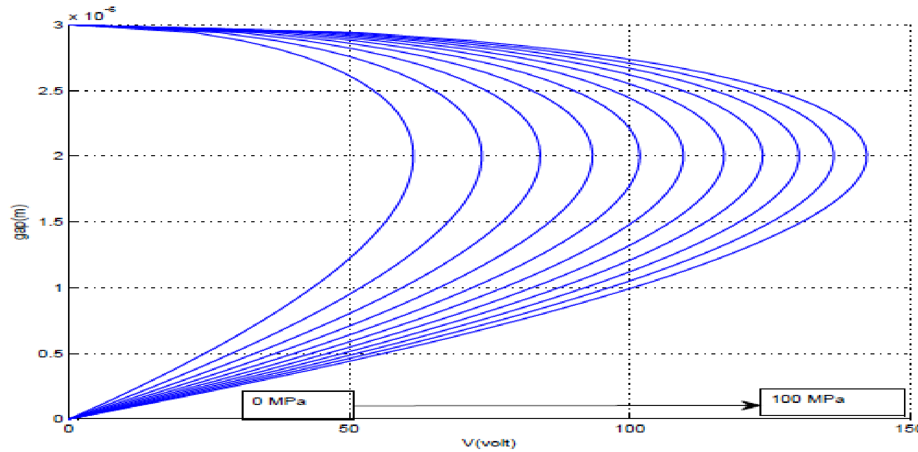

Fig. 5.3.Beam height versus applied voltage with W=100 µm, w=20 µm, go=3 µm and residual stress varying from 0MPa to 100 MPa in steps of 10MPa

This is because the beam becoming unstable at $2g_o/3$ which is due to positive feedback in the electrostatic actuation. At $2g_o/3$, the increase in electrostatic force is greater than the increase in the restoring force, resulting in (a) the beam position becoming unstable and (b) collapse of beam in down state position. Table 5.2 shows theoretical relation between pull down voltage , spring constant and the residual stress for the designed beam structure with g_0=3 µm.

Table 5.2:Relation between residual stress and Pull in voltage

Residual Stress[MPa]	Spring constant[N/m]	Pull in voltage(volt) at (2/3)go
0	8.3592	61.4668
10	12.0072	73.6680
20	15.6552	84.1177
30	19.3032	93.4056
40	22.9512	101.85
50	26.5992	109.6459
60	30.2472	116.9232
70	33.8952	123.7734
80	37.5432	130.2638
90	42.1912	136.4459
100	44.8392	142.3597

5.3. ELECTROMECHANICAL SIMULATION RESULTS

As per the requirement of the project , a fixed-fixed beam is suspended over a transmission line (CPW in this case) and is to be actuated in stable region, resulting in change in electrical length of the resonator. To simulation the design in coventor MEMS+[12], first process and the material properties are defined then the beam and electrode of required geometry are designed as shown in Fig.5.4(a),(b), and (c).

Coventor MEMS+ - E:/TRAINEE/ROHIT ASHISH TRAINEE/DISPLACEMENT MES.proc*

MaterialDataBase | ProcessEditor | ComponentLibrary | Innovator | Simulator | New3DSchematic.DC1 | New3DSchematic.DC1.Modal1.eig

Name	Layer Name	Material Name	Material Color	Thickness	Mask Name	Photoresist	Mask Offset	Sidewall Angle	Wafer Side	Gds Number
Substrate	Substrate	Silicon		270						
StackMaterial1	GOLEDLINE	Gold		1						
StraightCut1					GOLD CUT	Positive	0	0	Front	0
StackMaterial2	NITRIDE	SiliconNitride		0.2						
StraightCut2					DIELCTRIC CUT	Positive	0	0	Front	0
StackMaterial3	SRIFICIAL	Oxide		3						
StackMaterial4	GOLDBRIDGE	Gold		2						
StraightCut3					BRIDGE CUT	Positive	0	0	Front	0
DeleteStep1										

(a)

Coventor MEMS+ - C:/Coventor/MEMS+6/Examples/Mirror/MEMSpMaterialDatabase.mmdb*

MaterialDataBase | ProcessEditor | ComponentLibrary | Innovator | Simulator | New3DSchematic.DC1 | New3DSchematic

aterial List

- Material List
  - Air
  - Aluminum
  - AluminumNitride
  - Gold
  - Oxide
  - Polysilicon
  - Silicon
  - SiliconNitride
  - ThermalOxide
  - ZincOxide
  - LithiumNiobate

Name	Value	Units
Visual Properties		
Color	Yellow	
Transparency		
Material Orientation : Euler Angles (X,Y',Z'')		
Density	19300	kg/m^3
Elastic Constants : Isotropic		
Isotropic		
E	82.737	GPa
nu	0.44	
PreStress : In-plane Isotropic		
In-plane Isotropic		
Stress	22	MPa
Stress Gradient in Z : Anisotropic		
Anisotropic		
x	0	Pa/m
y	0	Pa/m
Thermal Coefficient of Expansion		
alpha	1.42e-05	1/K
Zero Stress Temperature	273.15	K
Thermal Conductivity	317	W/(m*K)
Specific Heat	129	J/(kg*K)
Electrical Conductivity	4.25532e+07	S/m
Piezoelectric Coefficients : Stress Coefficients		
Relative Permittivity : Isotropic		
Piezoresistive Coefficients		
Relative Permeability	undef	
Coercivity	undef	A/m
Saturation Magnetization	undef	A/m

(b)

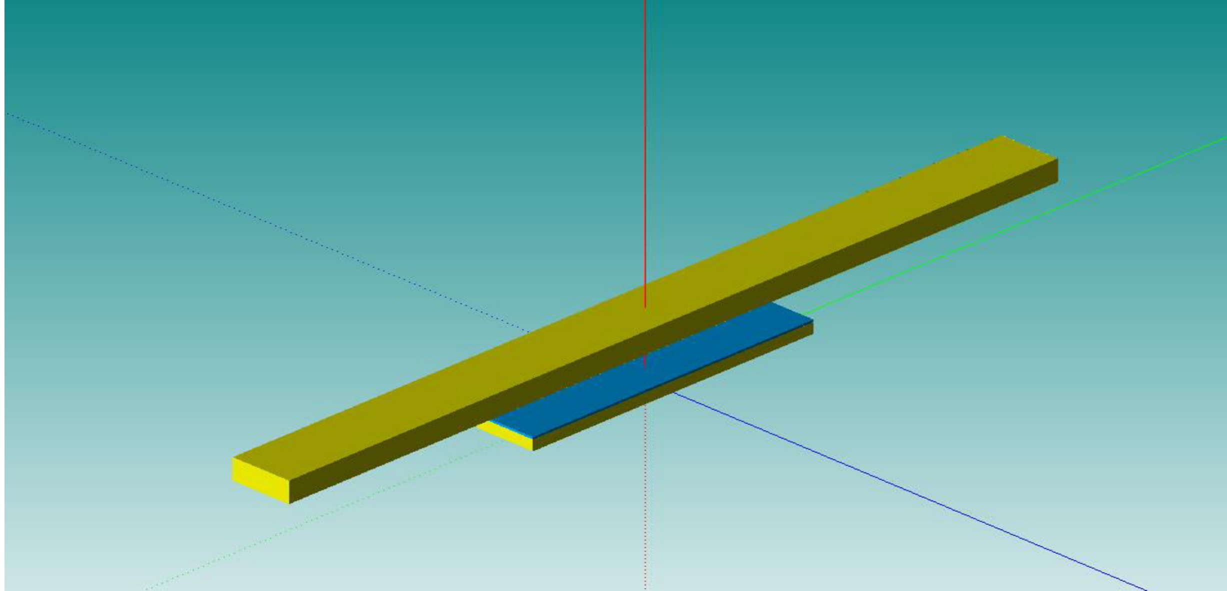

(c)

Fig.5.4.(a) Process definition of design (b) Material properties definition (c) Required actuator design

Like that various observations are made with different dielectric thickness, different air gap and for different length which has been tabulated in following tables.

Table5.3. Relation of displacement with applied voltage for given air gap

(a) l=300 µm, t_d=0.3, w x W=20 µm x 100 µm and σ = 0MPa

Air gap go(µm)	Voltage applied(volt)	Displacement(µm)
3	75(Pull-in voltage)	3
	72	1.02
	60	0.54
	55	0.43
	30	0.108
2	39(Pull-in voltage)	2
	37	0.58
	30	0.28
	22	0.132
	18	0.0848
1	14(Pull-in voltage)	1

	13	0.28
	10	0.12

(b) l=300 µm, t_d = 0.3µm, w x W= 20 µm x 100 µm and σ = 50MPa

Air gap go(µm)	Voltage applied(volt)	Displacement(µm)
2	70(Pull-in voltage)	2
	65	0.577
	52	0.264
	36	0.109

(c) l=300µm, t_d= 0.2µm, w x W= 20 µm x 100 µm and σ = 0MPa

Air gap go(µm)	Voltage applied(volt)	Displacement(µm)
3	72(Pull-in voltage)	2.9
	68	0.97
	55	0.478
	28	0.0998

(d) l=274 µm, t_d =0.2µm, w x W=20 µm x 100 µm and σ= 0MPa

Air gap go(µm)	Voltage applied(volt)	Displacement(µm)
3	87(Pull-in voltage)	3
	84	1.05
	80	0.852
	68	0.514
	52	0.263
	35	0.109

(e) l=274µm, t_d = 0.2µm, w x W= 20 µm x 100 µm and σ= 22MPa

Air gap go(µm)	Voltage applied(volt)	Displacement(µm)
3	111(Pull-in voltage)	3
	108	1.01

	104	0.834
	88	0.479
	70	0.267
	45	0.110

Table5.3(c) shows that for the beam as used in design, pull-in voltage is 72V i.e. less than 72V is required for actuation in stable region before pull down. Actuation voltage increases by approximately 30V if stress of 50MPa is considered for 300 µm long beam. It is noted that 300µm is the suitable length for the beam in terms of less actuation voltage and is less prone to self actuation. The displacement of 1 µm of the designed beam (g_0=3µm) has been shown in Fig. 5.5 actuation voltage of 70V.

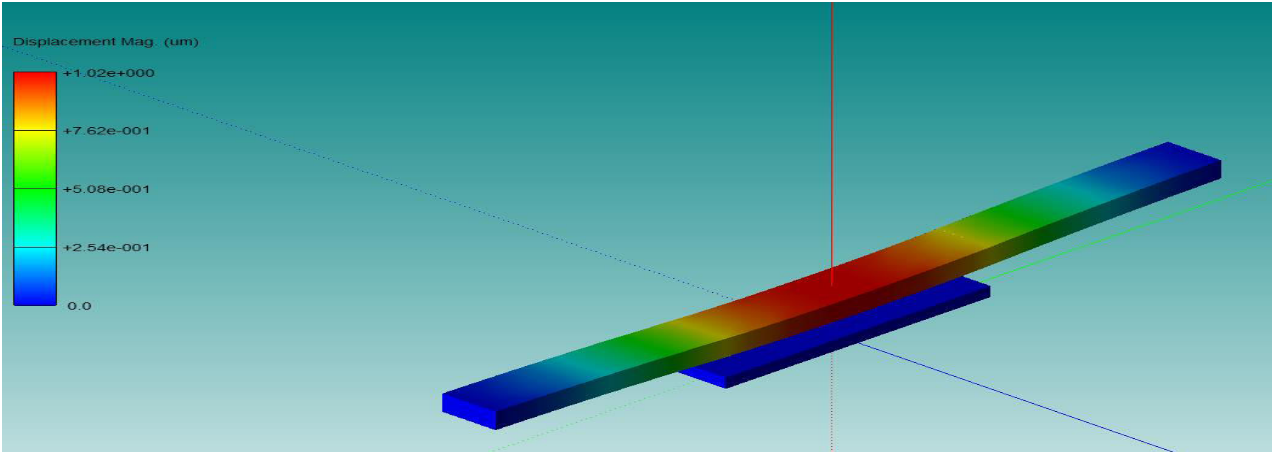

Fig.5.5. Dynamic view of beam in actuated state (w=20µm, actuation voltage=70V yields displacement of 1 µm i.e. g=2µm)

CHAPTER 6
RF SIMULATION OF THE FILTER

6.1 INTRODUCTION

This chapter highlights the RF analysis of the final design. As already stated in chapter 3, the basic filter structure consists of a CPW t-line periodically loaded with 12 MEMS capacitive shunt bridges corresponding to Bragg's frequency almost 10 times of central frequency. The bridge dimensions have been already optimized and the static and modal analyses are preformed in chapter 3 and chapter4 respectively. This chapter focuses on the final design and its RF characterization which has been carried out by means of Ansoft HFSS v.13, a FEM (Finite Element Method) based simulator for structures operating at a high-frequency range.

6.2 RF MEMS TUNABLE BAND PASS FILTER

6.2.1 DESIGN

Similar to the concept extended by the authors of the papers included in the review, but most of them are in K band around 20GHz. This work is aimed at extending the similar capacitively coupled DMTL resonator based design in lower frequency band in Ku band around 15 GHz. In this design, three cantilever parallel series bridges have been used to achieve coupling between resonators and beam length longer than the sum of width of central signal line and the gaps has been used. These have been done to achieve better loss characteristics and to lower the actuation voltage. Moreover two single pole resonators have been cascaded to achieve better out of band rejection. Electrical length and the coupling capacitance values have been given in chapter4.

Fig. 6.1 shows the final structure of the desired tunable filter. This structure has been simulated in Ansoft HFSS v13[11] and the corresponding insertion loss and return loss is noted for the possible tuning range. Summarizing all the design parameters of the DMTL resonator based filter designed, it is tabulated in Table 6.2

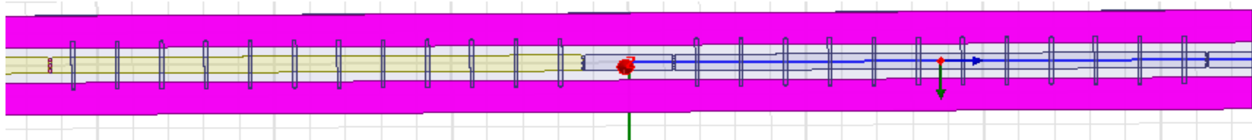

(a)

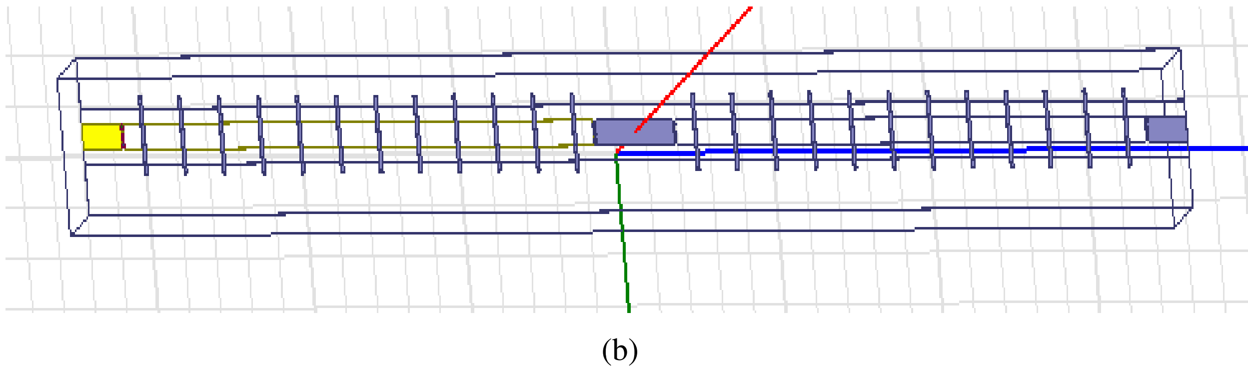

(b)

Fig.6.1.(a) Top view of the designed filter (b) Three dimensional view of the structure.

Table 6.1.Design parameters of capacitively coupled DMTL resonator

Parameters	**Materials Used**	**Dimension**(µm)
G/W/G of CPW Line	Gold (Au)	60/100/60
Substrate Thickness	Silicon (Si)	270
Thickness of Dielectric Layer(td)	Silicon Nitride(Si3N4)	0.2
Shunt Bridge Length(l)	Gold(Au)	300
Shunt Bridge Width(w)	Gold(Au)	20
Bridge Thickness(t_b)	Gold(Au)	2
No of bridges per resonator		12
Air Gap(g0)	Vacuum	3
Series Bridge width	Gold(Au)	20

6.2.2 RF CHARACTERIZATION BY HFSS v13 SIMULATION

This sections includes the loss-performance i.e., measurement of S11 and S21 in dB, Impedance variation, dielectric permittivity variation in tuning range. According to mechanical model, if shunt bridge is designed with 3 µm air gap then the stable displacement up to 1 µm can be achieved. Fig. 6.2 and Table 6.3 depict the S-parameters (dB) vs. Frequency (GHz) respectively for the possible tunable central frequencies.

OPTIMIZATION [1] RESULTS

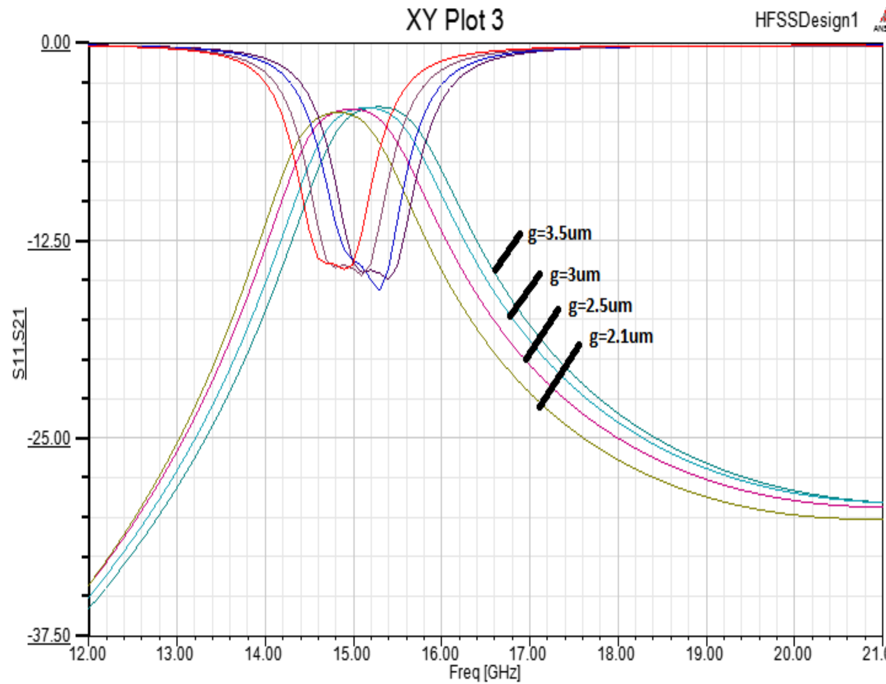

Fig.6.2. S-parameters (dB) vs. Frequency (GHz) (DMTL resonator length 3000 µm ,250 µm of 50Ω line and series cantilever bridge overlapping area 3x50 µm²)

Table 6.2.Relation of central frequency and losses with actuation

g_o(µm)	f_c(GHz)	S21(dB)	S11(dB)	10dB freq(GHz)		~30dBfreq(GHz)		10dB BW
2.1	14.8	-4.3878	-14.2081	14.0982	15.6231	12.5262	21(30.03dB)	10.30%
2.5	15	-4.2100	-14.5100	14.1945	15.8359	12.5558	21(29.50dB)	10.94%
3	15.2	-4.1181	-15.1800	14.3462	16.0348	12.6714	21(29.30dB)	11.11%

Table 6.3.Relation of capacitance and relative 3dB bandwidth with actuation

g_o(µm)	f_c(GHz)	Capacitance (fF)	S21(dB)	Relative 3dB freq(GHz)		Relative 3dB BW
2.1	14.8	11.171	-4.3878	14.2767	15.4036	7.614%
2.5	15	9.509	-4.2100	14.3876	15.5944	8.045%
3	15.2	8.313	-4.1181	14.5526	15.7750	8.042%

Simulated results demonstrate that 2.6 % tuning range can be achieved at 15 GHz .Table 6.3 shows how capacitance and relative 3dB bandwidth vary. Relative bandwidth varies from 7.6% to 8% in entire tuning range.

OPTIMIZATION [2] RESULTS

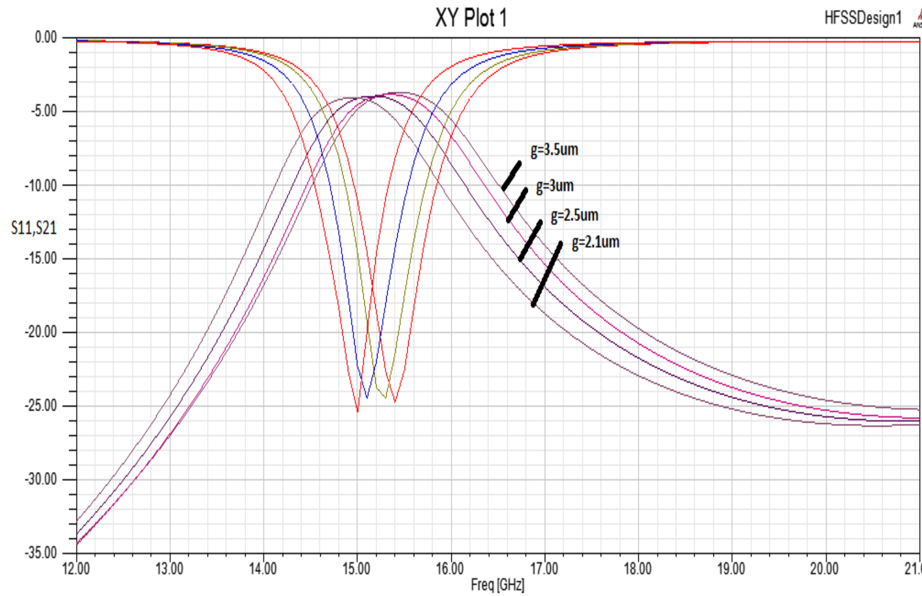

Fig. 6.3. S-parameters (dB) vs. Frequency (GHz) (DMTL resonator length 2850 µm , 490 µm of 50 Ω line and series cantilever bridge overlapping area 3x60 µm^2)

Table 6.4.Relation of central frequency and losses with actuation

g_o(µm)	f_c(GHz)	S21(dB)	S11(dB)	10dB freq(GHz)		~30dBfreq(GHz)		10dB BW
2.1	14.90	-4.1061	-25.2499	14.1220	15.8809	12.3636	21(26.22dB)	11.80%
2.5	15.15	-4.0053	-24.4400	14.3092	16.1429	12.5000	21(26.01dB)	12.10%
3	15.35	-3.8796	-24.4567	14.4598	16.3519	12.6200	21(25.78dB)	12.33%

Table 6.5.Relation of capacitance and relative 3dB bandwidth with actuation

g_o(µm)	f_c(GHz)	Capacitance (fF)	S21(dB)	Relative 3dB freq(GHz)		Relative 3dB BW
2.1	14.90	11.171	-4.1061	14.3457	15.5858	8.323%
2.5	15.15	9.509	-4.0053	14.5441	15.8280	8.475%
3	15.35	8.313	-3.8796	14.7082	16.0188	8.538%

Simulated results demonstrate that 2.932 % tuning range can be achieved at 15 GHz. Table 6.3 shows how capacitance and relative 3dB bandwidth vary. Relative bandwidth varies from 8.3% to 8.5% in entire tuning range. Best possible Insertion loss and return loss achieved are -0.8796dB at 15.35GHz and –24.2499dB at 14.9 GHz respectively.

CHAPTER 7
CONCLUSION AND SCOPE OF FUTURE WORK

7.1 CONCLUSIONS

This thesis reveals the designs and modeling aspect of a RF MEMS tunable band pass filter in Ku band around 15 GHz. The design employs miniaturized RF MEMS tunable capacitors, which are placed in shunt on a CPW t-line to yield an appreciable amount of change in electrical length of resonator resulting change in central frequency. A literature review, based on the papers published having certain relevance to the topic of this dissertation, is conducted. The capacitively coupled resonator based tunable filter is designed on a 270 μm thick silicon substrate(ε_r = 11.9).

As per first optimization, the overall filter dimension of designed MEMS tunable band pass filter is 0.62 mm× 6.5 mm. The simulated results demonstrate a tuning range from 14.8 GHz to15.2 GHz with -4.1dB minimum insertion losses. The relative 3 dB bandwidth is approximately 7.6 - 8%. and 10dB bandwidth varies from 10.30 - 11.11%. The tunability of 2.6% can be achieved at 15GHz. The 30dB rejection has been achieved around 12.5 GHz and 21GHz respectively. Return loss varies from -15.18 dB to -14.2 dB in pass band at all tuning ranges and the insertion loss varies from -4.4 to -4.1 dB.

As per second optimization, the overall filter dimension of designed MEMS tunable band pass filter is 0.62 mm× 7.7mm.The simulated results demonstrate a tuning range from 14.9 GHz to15.35 GHz with -3.88 dB minimum insertion losses. The relative 3 dB bandwidth is approximately 8.3 - 8.5% and 10dB bandwidth varies from 11.8 – 12.3%. The tunability of 2.9% can be achieved at 15.35GHz. The 30dB rejection has been achieved around 12.5 GHz and 21GHz respectively. Return loss varies from -25.24 dB to-24.45 dB in pass band at all tuning ranges and the insertion loss varies from -4.1 to -3.87dB.

The port impedance varies from 49.3 to 50.7 Ω over the tuning range. Capacitance between signal line and beam varies from 8.313 to 11.171fF. According to electromechanical simulation, the ideal actuation voltage required would be up to 70V for actuation in stable region. It has been

observed that better insertion and return loss can be achieved but on the cost of poor out of band rejection.

7.2 WORK TO BE CARRIED OUT AND ITS FUTURE SCOPES

The realization of the proposed design of the unit cell structure and the corresponding tunable band pass filter structures are to be fabricated and characterized to see whether the designed results and the results obtained after fabrication are in close approximation or not.

As its future is concerned, this design with some improvement can simplify the complexity of tunable band pass filter being used and can be used as tracking blocks for radiometers, radar system and telecommunication.

REFERENCES

[1] Gabriel M. Rebeiz "RF MEMS-Theory, Design & Technology" *Wiley Inter science*, A John Wiley & Sons Publication, September 2002 [Chapter 1, 2, 3, 4, 5, 10]

[2] Gabriel M. Rebeiz, Jeremy B. Muldavin, "RF MEMS Switches & Switch Circuits", *IEEE Microwave Magazine* 59, December 2001

[3] G Rezazadehl, H Sadeghian, E Malekpour, "A Comparison Simulation of Fixed-fixed Type MEMS Switches", Institute of Physics Publishing Journal of Physics ,Conference Series 34 (2006) 500–505 doi:10.1088/1742-6596/34/1/082 *International MEMS Conference* 2006

[4] Yu Liu, Andrea Borgioli, Amit S. Nagra, Robert A. York, "Distributed MEMS Transmission Lines for Tunable Filter Applications", Electrical and computer Engineering Department, University of California at Santa Barbara, California, *John Wiley and sons Inc*. 2001

[5] Tamijani, A. Dussopt and Rebeiz, "Miniature and tunable filter using MEMS capacitors", *IEEE Trans. Microwave Theory Tech*. 2003

[6] Brank J. Yao, Z.J. Eberly, M. Malczewski, A. Varian and Golsmith, "RF MEMS based tunable filter", *Int. J. RF Microwave Computer-Aided ENG* 276-284, September 2001

[7] David M. Pozar, "Microwave Engineering" 2nd edition, *John Wiely and sons Inc* [Chapter8]

[8] http://accessengineeringlibrary.com/

[9] http://www.keysight.com/en/pc-1297113/advanced-design-system

[10] http://www.matlab.com/

[11] http://www.ansoft.com/products/hf/hfss

[12] http://www.coventor.com/